

To appear in *Protostars and Planets IV*, eds. V. Mannings, A.P. Boss, and S.S. Russell (Tucson: Univ. of Arizona Press) – Accepted 1999 January –

FROM PRE-STELLAR CORES TO PROTOSTARS: THE INITIAL CONDITIONS OF STAR FORMATION

PHILIPPE ANDRÉ

CEA/DSM/DAPNIA, Service d'Astrophysique, Saclay, France

DEREK WARD-THOMPSON

University of Wales, Cardiff, UK

and

MARY BARSONY

University of California at Riverside

The last decade has witnessed significant advances in our observational understanding of the earliest stages of low-mass star formation. The advent of sensitive receivers on large radio telescopes such as the JCMT and IRAM 30m MRT has led to the identification of young protostars at the beginning of the main accretion phase ('Class 0' objects), and has made it possible to probe, for the first time, the inner density structure of pre-collapse cores. Class 0 objects are characterized by strong, centrally-condensed dust continuum emission at submillimeter wavelengths, very little emission shortward of $\sim 10 \mu\text{m}$, and powerful jet-like outflows. Direct evidence for gravitational infall has been observed toward several of them. They are interpreted as accreting protostars which have not yet accumulated the majority of their final stellar mass. In contrast to protostars, pre-stellar cores have flat inner density profiles, suggesting the initial conditions for fast protostellar collapse depart sometimes significantly from a singular isothermal sphere. In the case of non-singular initial conditions, the beginning of protostellar evolution is expected to feature a brief phase of vigorous accretion/ejection which may coincide with Class 0 objects. In addition, submillimeter continuum imaging surveys of regions of multiple star formation such as Ophiuchus and Serpens suggest a picture according to which each star in an embedded cluster is built from a finite reservoir of mass and the associated IMF is primarily determined at the pre-stellar stage of evolution.

I. INTRODUCTION

The formation of low-mass stars is believed to involve a series of conceptually different stages (e.g. Larson 1969, Shu, Adams, & Lizano 1987). The first stage corresponds to the fragmentation of a molecular cloud into a number of gravitationally-bound cores which are initially supported against gravity by a combination of thermal, magnetic, and

turbulent pressures (e.g. Mouschovias 1991, Shu et al. 1987). These pre-stellar condensations/fragments form and evolve as a result of a still poorly understood mechanism, involving ambipolar diffusion (e.g. Mouschovias 1991), the dissipation of turbulence (e.g. Nakano 1998), and/or an outside impulse (e.g. Bonnell et al. 1997). Once such a condensation becomes gravitationally unstable and collapses, the main *theoretical* features of the ensuing dynamical evolution have been known since the pioneering work of Larson (1969). During a probably brief initial phase, the released gravitational energy is freely radiated away and the collapsing fragment stays roughly isothermal. This “runaway” isothermal collapse phase tends to produce a strong central concentration of matter with a radial density gradient approaching $\rho \propto r^{-2}$ at small radii essentially independently of initial conditions (e.g. Whitworth & Summers 1985, Blottiau et al. 1988, Foster & Chevalier 1993). It ends with the formation of an opaque, hydrostatic protostellar object in the center (e.g. Larson 1969, Boss & Yorke 1995, Bate 1998). Numerical simulations in fact predict the successive formations of two hydrostatic objects, before and after the dissociation of molecular hydrogen respectively (see Boss & Yorke 1995), but we will not distinguish between them here. One then enters the main accretion phase during which the central object builds up its mass (M_*) from a surrounding infalling envelope (of mass M_{env}) and accretion disk, while progressively warming up. In this chapter, we will refer to the system consisting of the central object, plus envelope and disk as an accreting protostar. The youngest accreting protostars have $M_{env} \gg M_*$, and radiate the accretion luminosity $L_{acc} \approx GM_*\dot{M}_{acc}/R_*$. In the ‘standard’ theory of isolated star formation (Shu et al. 1987, 1993), the collapse initial conditions are taken to be (static) singular isothermal spheroids ($\rho \sim (a^2/2\pi G)r^{-2}$, cf. Li & Shu 1996, 1997), there is no runaway collapse phase, and the accretion rate \dot{M}_{acc} is constant in time $\sim a^3/G$, where a is the effective isothermal sound speed. With other collapse initial conditions, the accretion rate is generally time-dependent (see III–D below).

Observations have shown that the main accretion phase is always accompanied by a powerful ejection of a small fraction of the accreted material in the form of prominent bipolar jets/outflows (e.g. Bachiller 1996). These outflows are believed to carry away the excess angular momentum of the infalling matter (e.g. Königl & Pudritz, this volume). When the central object has accumulated most ($\gtrsim 90\%$) of its final, main-sequence mass, it becomes a pre-main sequence (PMS) star, which evolves approximately at fixed mass on the Kelvin-Helmholtz contraction timescale (e.g. Stahler & Walter 1993). (Note that, during the protostellar accretion phase, stars more massive than a few $0.1 M_\odot$ start burning deuterium, while stars with masses in excess of $\sim 8 M_\odot$ begin to burn hydrogen – see Palla & Stahler 1991.)

The details of the earliest stages outlined above are still poorly known. Improving our understanding of these early stages is of prime importance since to some extent they must govern the origin of the stellar initial mass function (IMF).

Observationally, it is by comparing the structure of starless dense cores with that of the envelopes surrounding the youngest stellar objects that one may hope to estimate the initial conditions for protostellar collapse. The purpose of this chapter is to review several major advances made in this field over the last decade, thanks mostly to ground-based (sub)millimeter continuum observations. We discuss results obtained on pre-stellar cores and young accreting protostars in Sect. II and Sect. III, respectively. We then combine these two sets of results and conclude in Sect. IV.

II. PRE-STELLAR CORES

A. Definition and Identification

The pre-stellar stage of star formation may be defined as the phase in which a gravitationally bound core has formed in a molecular cloud, and evolves toward higher degrees of central condensation, but no central hydrostatic protostellar object exists yet within the core.

A pioneering survey of isolated dense cores in dark clouds was carried out in transitions of NH_3 by Myers and co-workers (see Myers & Benson 1983, Benson & Myers 1989 and references therein), who catalogued about 90 cores. These were separated into starless cores and cores with stars (Beichman et al. 1986), on the basis of the presence or absence of an embedded source detected by IRAS. The starless NH_3 cores were identified by Beichman et al. as the potential sites of future isolated low-mass star formation. Other dense core surveys have been carried out by Clemens & Barvainis (1988), Wood et al (1994), Bourke et al (1995a,b), Lee & Myers (1999), and Jessop & Ward-Thompson (1999).

Using the 15 m James Clerk Maxwell Telescope (JCMT), Ward-Thompson et al. (1994) observed the 800- μm dust continuum emission from about 20 starless NH_3 cores from the Benson & Myers list, mapping 4 of the cores, and showed that they have larger FWHM sizes than, but comparable masses to the envelopes of the youngest protostars (Class 0 sources – see III below). This is consistent with starless NH_3 cores being pre-stellar in nature and the precursors of protostars (see also Mizuno et al. 1994). Ward-Thompson et al. also demonstrated that pre-stellar cores do not have density profiles which can be modelled by a single scale-free power law, but instead have flat inner radial density profiles, suggestive of magnetically-supported cores contracting by ambipolar diffusion (see Mouschovias 1991, 1995 and

references therein). Recent molecular line spectroscopy of several pre-stellar cores (e.g. Tafalla et al. 1998 and Myers et al. this volume) appears to support the argument that they are contracting, but more slowly than the infall seen toward Class 0 protostars (e.g. Mardones et al. 1997 – see III–C).

The 800 μm study by Ward-Thompson et al. (1994) also suggests that wide-field submillimeter continuum imaging may be a powerful tool to search for new pre-stellar cores in the future (cf. Ristorcelli et al. 1998).

B. Spectral Energy Distributions and Temperatures

The advent of the Infrared Space Observatory (ISO) of the European Space Agency (ESA), has allowed pre-stellar cores to be studied in the far-infrared for the first time (Ward-Thompson et al. 1999a in prep), since these cores were not detected by IRAS. Likewise, the Submillimetre Common User Bolometer Array (SCUBA) camera on the JCMT has allowed pre-stellar cores to be observed in the submm with greater signal to noise than ever before (Ward-Thompson et al. 1999b in prep). Pre-stellar cores emit almost all of their radiation in the FIR/submm/mm regimes, so the combination of these two instruments provides a unique opportunity to study them.

As an illustration, Figure 1 shows a series of images of the L1544 pre-stellar core at 90 & 200 μm (from ISO), 850 μm (from SCUBA), and 1.3 mm (from IRAM). The core is clearly detected at 200–1300 μm , but is almost undetected at 90 μm . This shows that the core is very cold, and its dust temperature can be obtained from fitting a modified black-body to the observed emission. The spectral energy distribution (SED) of L1544 in the far-infrared and submillimeter wavelength regimes is shown in Fig. 2. The solid line is a grey-body curve of the form:

$$S_\nu = B_\nu(T_{dust}) [1 - \exp(-\tau_\nu)] \Delta\Omega,$$

where $B_\nu(T_{dust})$ is the Planck function at frequency ν for a dust temperature T_{dust} , $\tau_\nu = \kappa_\nu \Sigma$ is the dust optical depth through a mass column density Σ (see below), and $\Delta\Omega$ is the source solid angle. In this simple modelling, the dust opacity per unit (gas + dust) mass column density, κ_ν , is assumed to scale as ν^β with $\beta = 1.5\text{--}2$ as usually appropriate in the submillimeter range (e.g. Hildebrand 1983). For L1544, a good fit to the SED is obtained with $T_{dust} = 13$ K and $\beta = 2$. Similar results are obtained in other starless cores. This confirms the lack of any warm dust in such cores, and consequently the lack of any embedded protostellar object. The (sub)millimeter data show a morphology similar to the ISO images, at much higher resolution, indicating that the same dust is being observed at all wavelengths. Consequently the temperature derived from the SED is representative of all the emitting dust and can be used to convert submillimeter fluxes into estimates of

dust masses, and hence to gas masses.

C. Mass and Density Structure

Dust emission is generally optically thin at (sub)millimeter wavelengths, and hence is a direct tracer of the mass content of molecular cloud cores. For an isothermal dust source, the total (gas + dust) mass $M(r < R)$ contained within a radius R from the center is related to the submillimeter flux density $S_\nu(\theta)$ integrated over a circle of projected angular radius $\theta = R/d$ by:

$$M(r < R) \equiv \pi R^2 \langle \Sigma \rangle_R = [S_\nu(\theta) d^2] / [\kappa_\nu B_\nu(T_{dust})],$$

where $\langle \Sigma \rangle_R$ is the average mass column density. The dust opacity κ_ν is somewhat uncertain, but the uncertainties are much reduced when appropriate dust models are used (see Henning et al. 1995 for a review). For pre-stellar cores of intermediate densities ($n_{H_2} \lesssim 10^5 \text{ cm}^{-3}$), κ_ν is believed to be close to $\kappa_{1.3} = 0.005 \text{ cm}^2 \text{ g}^{-1}$ at 1.3 mm (e.g. Hildebrand 1983, Preibisch et al. 1993). In denser cloud cores and protostellar envelopes, grain coagulation and the formation of ice mantles make κ_ν a factor of ~ 2 larger, i.e., $\kappa_{1.3} = 0.01 \text{ cm}^2 \text{ g}^{-1}$ assuming a gas-to-dust mass ratio of 100 (e.g. Ossenkopf & Henning 1994). A still higher value, $\kappa_{1.3} = 0.02 \text{ cm}^2 \text{ g}^{-1}$, is recommended in protoplanetary disks (Beckwith et al. 1990, Pollack et al. 1994).

Following this method, FWHM masses ranging from $\sim 0.5 M_\odot$ to $\sim 35 M_\odot$ are derived for the 9 isolated cores mapped by Ward-Thompson, Motte, & André (1999 – hereafter WMA99).

Although observed pre-stellar cores are generally not circularly or elliptically symmetric (see, e.g., Fig. 1), one can still usefully constrain their radial density profiles by averaging the (sub)millimeter emission in circular or elliptical annuli.

Figure 3a shows the azimuthally-averaged radial intensity profile of the pre-stellar core L1689B at 1.3 mm, compared to the profile of a spherical isothermal core model with $\rho(r) \propto r^{-2}$. The model intensity profile results from a complete simulation taking into account both the observing technique (dual-beam mapping) and the reduction method (cf. André, Ward-Thompson, & Motte 1996). We see that L1689B exhibits the familiar radial profile of pre-stellar cores, with a flat inner region, steepening toward the edges (Ward-Thompson et al. 1994, André et al. 1996, WMA99). In this representative example, the radial density profile inferred assuming a constant dust temperature is as flat as $\rho(r) \propto r^{-0.4}$ (if the 3-D core shape is disk-like) or $\rho(r) \propto r^{-1.2}$ (if the core shape is spheroidal) at radii less than $R_{flat} \sim 4000 \text{ AU}$, and approaches $\rho(r) \propto r^{-2}$ only between $\sim 4000 \text{ AU}$ and $\sim 15000 \text{ AU}$.

More recently, it has been possible to constrain the outer density gradient of starless cores through *absorption* studies in the mid-infrared with ISOCAM (e.g. Abergel et al. 1996, 1998, Bacmann et al. 1998). It

appears that isolated pre-stellar cores are often characterized by sharp edges, steeper than $\rho \propto r^{-3}$ or $\rho \propto r^{-4}$, at radii $R \gtrsim 15000$ AU.

These features of pre-stellar density structure, i.e., inner flattening and sharp outer edge, are qualitatively consistent with models of magnetically-supported cores evolving through ambipolar diffusion prior to protostar formation (e.g. Ciolek & Mouschovias 1994, Basu & Mouschovias 1995), although the models generally require fairly strong magnetic fields ($\sim 100 \mu\text{G}$). Alternatively, the observed structure may also be explained by models of thermally supported self-gravitating cores interacting with an external UV radiation field (e.g. Falgarone & Puget 1985, Chièze & Pineau des Forêts 1987).

D. Lifetimes

Beichman et al. (1986) used the ratio of numbers of starless cores to numbers of cores with embedded IRAS sources to estimate their relative timescales. They found roughly equal numbers of cores with and without IRAS sources. They estimated the lifetime of the stage of cores with stars, based on T Tauri lifetimes and pre-main sequence HR diagram tracks (e.g. Stahler 1988). Based on this, they estimated the lifetime of the pre-stellar core phase to be a few times 10^6 yr.

However, the lifetime of a pre-stellar core depends on its central density. Figure 4 (taken from Jessop & Ward-Thompson 1999) shows the estimated lifetime of starless cores for each of six dark cloud surveys mentioned in II-A above, versus the mean volume density of cores in each sample. The lifespan of cores without stars in each sample was estimated from the fraction of cores with IRAS sources, using the same method as Beichman et al. (1986). An anti-correlation between lifetime and density is clearly apparent in Fig. 4. The solid line has the form $t \propto \rho^{-0.75}$, while the dashed line is of the form $t \propto \rho^{-0.5}$. These two forms are expected for cores evolving on the ambipolar diffusion timescale $t_{AD} \propto x_e$ (where x_e is the ionisation fraction – e.g. Nakano 1984), if the dominant ionisation mechanism is cosmic ray ionisation or UV ionisation, respectively (e.g. McKee 1989).

More details about the evolution of pre-stellar cores at higher densities can be inferred from the results of the submm continuum SCUBA survey of Ward-Thompson et al. (1999b). In this survey, 17 of the 38 NH_3 cores without IRAS sources from Benson & Myers (1989) were detected by SCUBA at $850 \mu\text{m}$. Ward-Thompson et al. (1999b) estimate that the 17 SCUBA detections all have central densities between $\sim 10^5 \text{cm}^{-3}$ and $\sim 10^6 \text{cm}^{-3}$, whilst the 21 non-detections must have lower central densities, typically between $\sim 10^4 \text{cm}^{-3}$ and $\sim 10^5 \text{cm}^{-3}$ (see Benson & Myers 1989, Butner et al. 1995, and references therein). Consequently, they deduce that the lifetime of these two phases – central density increasing from $\sim 10^4 \text{cm}^{-3}$ to $\sim 10^5 \text{cm}^{-3}$ compared to central density of $\sim 10^5 \text{cm}^{-3}$ until the formation of a protostellar object

at the center – must be roughly equal. This can be compared with the predictions of ambipolar diffusion models.

Figure 3b is taken from Ciolek & Mouschovias (1994) and shows the radial density profile predicted by an ambipolar diffusion model at different evolutionary stages (t_0 to t_6). The stage at which the central density is $\sim 10^4 \text{cm}^{-3}$ corresponds to time t_1 and the stage at which the central density is $\sim 10^5 \text{cm}^{-3}$ corresponds to time t_2 . The time at which a protostellar object forms is effectively t_6 . In this model the time taken to go from t_1 to t_2 ($\sim 2 \times 10^6$ yr) is six times longer than the time taken to go from t_2 to t_6 . Some discrepancy could perhaps be accounted for by the statistical errors associated with our source number counting technique, but the ratio between the two timescales should be fairly robust: The model predicts that SCUBA should only have detected $\sim 1/7$ of the cores, whereas it detected half of the sample.

We are left with the conclusion that *cores at central densities of order $\sim 10^5 \text{cm}^{-3}$ evolve more slowly than ambipolar diffusion models predict* – i.e. the cores experience more support than a simple static magnetic field can provide. The extra support could perhaps be provided by turbulence which generates non-static magnetic fields (e.g. Gammie & Ostriker 1996, Nakano 1998, Balsara et al. 1998).

E. Pre-Stellar Condensations in Star-Forming Clusters

In regions of multiple star formation, submillimeter dust continuum mapping has revealed a wealth of small-scale cloud fragments, sometimes organized along filaments (e.g. Mezger et al. 1992, AWB93, Casali et al. 1993, Launhardt et al. 1996, Chini et al. 1997b, Johnstone & Bally 1999). Such fragmentation along filaments has not been observed in Taurus, but examples do exist in young embedded clusters forming primarily low-mass stars like ρ Ophiuchi (Motte, André, & Neri 1998). The individual fragments, which are denser ($\langle n \rangle \gtrsim 10^6 - 10^7 \text{cm}^{-3}$) and more compact (a few 1000 AU in size) than the isolated pre-stellar cores discussed above, often remained totally undetected (in emission) by *IRAS* or *ISO* in the mid- to far-IR. Since molecules tend to freeze out onto dust grains at low temperatures and high densities, (sub)millimeter dust emission may be the most effective tracer of such condensations (e.g. Mauersberger et al. 1992).

The most centrally-condensed of these starless fragments have been claimed to be isothermal protostars, i.e., collapsing condensations with no central hydrostatic object (see I) (e.g. Mezger et al. 1992, Launhardt et al. 1996, Motte et al. 1998). Good examples are FIR 3 and FIR 4 in NGC 2024, OphA-SM1 and OphE-MM3 in ρ Oph, LBS 17-SM in Orion B, or MMS1 and MMS4 in OMC-3. This isothermal protostar interpretation remains to be confirmed, however, by observations of appropriate spectral line signatures (cf. Myers et al. this volume).

Furthermore, the advent of large-format bolometer arrays now

makes possible systematic studies of the genetic link between pre-stellar cloud fragments and young stars. Figure 5 is a 1.3 mm continuum wide-field mosaic of the ρ Oph cloud (Motte et al. 1998) showing a total of 100 structures with characteristic angular scales of $\sim 15''$ – $30''$ (i.e., ~ 2000 – 4000 AU), which are associated with 59 starless condensations (undetected by ISO in the mid-IR) and 41 embedded YSOs (detected at IR or radio continuum wavelengths).

Comparison of the masses derived from the 1.3 mm continuum (from $\sim 0.05M_{\odot}$ to $\sim 3M_{\odot}$) with Jeans masses suggests that most of the 59 starless fragments are close to gravitational virial equilibrium with $M/M_{vir} \gtrsim 0.3$ – 0.5 and will form stars in the near future. These pre-stellar condensations generally have flat inner density profiles like isolated pre-stellar cores, but are distinguished by compact, finite sizes of a few thousand AU. The typical fragmentation lengthscale derived from the average projected separation between condensations is ~ 6000 AU in ρ Oph. This is ~ 5 times smaller than the radial extent of isolated dense cores in the Taurus cloud (see Gómez et al. 1993).

Figure 6 shows the mass distribution of the 59 ρ Oph pre-stellar fragments. It follows approximately $\Delta N/\Delta M \propto M^{-1.5}$ below $\sim 0.5M_{\odot}$, which is similar to the clump mass spectrum found by large-scale molecular line studies (e.g. Blitz 1993 and Williams et al. this volume). The novel feature, however, is that the fragment mass spectrum found at 1.3 mm in ρ Oph appears to steepen to $\Delta N/\Delta M \propto M^{-2.5}$ above $\sim 0.5M_{\odot}$. A similarly steep mass spectrum above $\sim 0.5M_{\odot}$ was obtained by Testi & Sargent (1998) for compact 3 mm starless condensations in the Serpens core. These pre-stellar mass spectra resemble the shape of the *stellar* initial mass function (IMF), which is known to approach $\Delta N/\Delta M_{\star} \propto M_{\star}^{-2.7}$ for $1 M_{\odot} \lesssim M_{\star} \lesssim 10 M_{\odot}$ and $\Delta N/\Delta M_{\star} \propto M_{\star}^{-1.2}$ for $0.1 M_{\odot} \lesssim M_{\star} \lesssim 1 M_{\odot}$ (e.g. Kroupa et al. 1993, Tinney 1993, 1995, Scalo 1998, see also Meyer et al. this volume). Given the factor of ~ 2 uncertainty on the measured pre-stellar masses, such a resemblance is remarkable and suggests that *the IMF of embedded clusters is primarily determined at the pre-stellar stage of star formation* (see also IV below).

III. THE YOUNGEST PROTOSTARS

A. Class 0 Protostars and Other YSO Stages

1. *Infrared YSO classes.* In the near-/mid-infrared, three broad classes of young stellar objects (YSOs) can be distinguished based on the slope $\alpha_{IR} = d\log(\lambda F_{\lambda})/d\log(\lambda)$ of their SEDs between $2.2 \mu\text{m}$ and 10 – $25 \mu\text{m}$, which are interpreted in terms of an evolutionary sequence (Lada & Wilking 1984, Lada 1987). Going backward in time, Class III ($\alpha_{IR} < -1.5$) and Class II ($-1.5 < \alpha_{IR} < 0$) sources correspond to

PMS stars (“Weak” and “Classical” T Tauri stars, respectively) surrounded by a circumstellar disk (optically thin and optically thick at $\lambda \lesssim 10 \mu\text{m}$, respectively), but lacking a dense circumstellar envelope (see André & Montmerle 1994 – hereafter AM94). The youngest YSOs detected at $2 \mu\text{m}$ are the Class I sources, which are characterized by $\alpha_{\text{IR}} > 0$ (e.g. Wilking, Lada, & Young 1989 – WLY89), and the close association with dense molecular gas (e.g. Myers et al. 1987). Class I objects are now interpreted as relatively evolved protostars with typical ages $\sim 1\text{--}2 \times 10^5$ yr (e.g. Barsony & Kenyon 1992, Greene et al. 1994, Kenyon & Hartmann 1995), surrounded by both a disk and a diffuse circumstellar envelope of substellar ($\lesssim 0.1\text{--}0.3 M_{\odot}$) mass (Whitney & Hartmann 1993, Kenyon et al. 1993b, AM94, Lucas & Roche 1997). Their SEDs are successfully modeled in the framework of the “standard” theory of isolated protostars (e.g. Adams, Lada, & Shu 1987, Kenyon et al. 1993a), in agreement with the idea that they derive a substantial fraction of their luminosity from accretion (see also Greene & Lada 1996 and Kenyon et al. 1998).

2. Class 0 protostars. Several condensations detected in submillimeter dust continuum maps of molecular clouds (e.g. II–E) appear to be associated with formed, hydrostatic YSOs and have been designated “Class 0” protostars (André, Ward-Thompson, & Barsony 1993 – AWB93). Specifically, Class 0 objects are defined by the following observational properties (AWB93):

- (i) Indirect evidence for a central YSO, as indicated by, e.g., the detection of a compact centimeter radio continuum source, a collimated CO outflow, or an internal heating source.
- (ii) Centrally peaked but extended submillimeter continuum emission tracing the presence of a spheroidal circumstellar dust envelope (as opposed to just a disk).
- (iii) High ratio of submillimeter to bolometric luminosity suggesting the envelope mass exceeds the central stellar mass: $L_{\text{smm}}/L_{\text{bol}} > 0.5\%$, where L_{smm} is measured longward of $350 \mu\text{m}$. In practice, this often means a SED resembling a single temperature blackbody at $T \sim 15\text{--}30$ K (see Fig. 2).

Property (i) distinguishes Class 0 objects from the pre-stellar cores and condensations discussed in Sect. II. In particular, deep VLA observations reveal no compact radio continuum sources in the centers of pre-stellar cores (Bontemps 1996, Yun et al. 1996). Properties (ii) and (iii) distinguish Class 0 objects from more evolved (Class I and Class II) YSOs. As shown by AWB93, the $L_{\text{smm}}/L_{\text{bol}}$ ratio should roughly track the ratio M_{env}/M_{\star} of envelope to stellar mass, and may be used as an evolutionary indicator (decreasing with time), for low-luminosity ($L_{\text{bol}} \lesssim 50 L_{\odot}$) embedded YSOs. Criterion (iii) approximately selects objects which have $M_{\text{env}}/M_{\star} > 1$, assuming plausible relations be-

tween L_{bol} and M_* on the one hand and between L_{smm} and M_{env} on the other hand (see AWB93 and AM94). [A roughly equivalent criterion is $M_{env}/L_{bol} > 0.1 M_{\odot}/L_{\odot}$.] *Class 0 objects are therefore excellent candidates for being very young accreting protostars in which a hydrostatic core has formed but not yet accumulated the majority of its final mass.* In practice, most of the confirmed Class 0 objects listed in Table 1 have $L_{smm}/L_{bol} \gg 0.5\%$ and are likely to be at the beginning of the main accretion phase with $M_{env} \gg M_*$ (see Fig. 7b).

3. Evolutionary diagrams for embedded YSOs. Combining infrared and submillimeter data, it is therefore possible to define a complete, empirical evolutionary sequence (Class 0 \rightarrow Class I \rightarrow Class II \rightarrow Class III) for low-mass YSOs, which likely correspond to conceptually different stages of evolution: (early) main accretion phase, late accretion phase, PMS stars with protoplanetary disks, PMS stars with debris disks (see AM94). This sequence is quasi-continuous and may be parameterized by the “bolometric temperature”, T_{bol} , defined by Myers & Ladd (1993) as the temperature of a blackbody having the same mean frequency as the observed YSO SED. Myers & Ladd proposed to use the $L_{bol}-T_{bol}$ diagram for embedded YSOs as a direct analog to the H-R diagram for optically visible stars. As shown by Chen et al. (1995, 1997), YSOs with known classes have distinct ranges of T_{bol} : < 70 K for Class 0, 70–650 K for Class I, 650–2880 K for Class II, and > 2880 K for Class III (e.g. Fig. 7a). The evolution of T_{bol} and L_{bol} from the Class 0 stage to the zero-age main sequence has been modelled in the context of various envelope-dissipation scenarios by Myers et al. (1998).

A perhaps more direct approach to tracking the circumstellar evolution of YSOs is to use the circumstellar mass $M_{c\star}$ derived from (sub)millimeter continuum measurements of optically thin dust emission. Such measurements show that $M_{c\star}$ ($= M_{env} + M_{disk}$) is generally dominated by M_{env} in Class 0/Class I sources (e.g. Terebey et al. 1993) and decreases by a factor ~ 5 –10 on average from one YSO class to the next (AM94). In the spirit of the L_{smm}/L_{bol} evolutionary indicator of AWB93, Saraceno et al. (1996a) proposed the $L_{smm}-L_{bol}$ (or equivalently $M_{env}-L_{bol}$) diagram as an alternative evolutionary diagram for self-embedded YSOs. While L_{smm} and M_{env} are well correlated with L_{bol} for the majority of embedded YSOs (e.g. Reipurth et al. 1993), Class 0 objects clearly stand out from Class I sources in this diagram as objects with excess (sub)millimeter emission, i.e., excess circumstellar material (see Fig. 7b). Moreover, one may compare the locations of observed embedded sources in the $M_{env}-L_{bol}$ diagram with simple protostellar evolutionary tracks (Saraceno et al. 1996a,b). Qualitatively at least, scenarios in which the mass-accretion rate decreases with time for a given protostar (Bontemps et al. 1996a, Myers et al. 1998 – see also III–D below) and increases with the mass of the initial pre-collapse

fragment (e.g. Myers & Fuller 1993, Reipurth et al. 1993, Saraceno et al. 1996b) yield tracks in better agreement with observations than the constant-rate scenario discussed by Saraceno et al. (1996a). In particular, the peak accretion luminosity is reduced by a factor $\sim 2-4$ compared to the constant-rate scenario (cf. Bontemps et al. 1996a, Myers et al. 1998, and Fig. 7b), which agrees better with observed luminosities (e.g. Kenyon & Hartmann 1995).

Inclination effects may a priori affect the positions of individual protostellar objects in these evolutionary diagrams. In particular, it has been claimed that some Class I sources may potentially look like Class 0 objects when observed at high inclination angles to the line of sight (e.g. Yorke, Bodenheimer, & Laughlin 1995, Sonnhalter, Preibisch, & Yorke 1995, Men'shchikov & Henning 1997). However, the fact that Class 0 objects are associated with an order of magnitude more powerful outflows than Class I sources (see III-D below) confirm that these two types of YSOs differ qualitatively from each other. Furthermore, some Class 0 sources are known to have small inclination angles (e.g. Cabrit & Bertout 1992, Greaves et al. 1997, Wolf-Chase et al. 1998). We also stress that existing (sub)millimeter maps of dust continuum and $C^{18}O$ emission provide direct evidence that both Class I and Class 0 objects are *self-embedded* in substantial amounts of circumstellar material distributed in spatially resolved, spheroidal envelopes (e.g. AM94, Chen et al. 1997, Ladd et al. 1998, Dent et al. 1998 – see also III-B below). This material has the ability to absorb the optical and near-IR emission from the underlying star/disk system and to reradiate it quasi-isotropically at longer far-IR and (sub)mm wavelengths. In such a self-embedded configuration, viewing-angle effects are minimized, as confirmed by radiative transfer calculations (e.g. Efstathiou & Rowan-Robinson 1991, Yorke et al. 1995). Physically, this is because the bulk of the luminosity emerges at long wavelengths where most of the emission is effectively optically thin. However, the short-wavelength emission from the inner star/disk remains very dependent on viewing angle, implying that T_{bol} estimates should be somewhat more sensitive to orientation effects than L_{bol} and L_{smm}/L_{bol} .

4. Protostar surveys and lifetime estimates. Based on the key attributes of Class 0 protostars (see 2. above), various strategies can be used to search for and discover new candidates: (sub)millimeter continuum mapping (e.g. Mezger et al. 1992, Casali et al. 1993, Sandell & Weintraub 1994, Reipurth et al. 1996, Launhardt et al. 1996, Chini et al. 1997ab, Motte et al. 1998, André et al. 1999), HIREs processing of the IRAS data (Hurt & Barsony 1996, O'Linger et al. 1999), deep radio continuum VLA surveys (e.g. Leous et al. 1991, Bontemps et al. 1995, Yun et al. 1996, Moreira et al. 1997, Gibb 1999), CO mapping (e.g. Bachiller et al. 1990, André et al. 1990, Bourke et al. 1997), and

large-scale near-IR/optical imaging of shocked H₂ and [SII] emission (e.g. Hodapp & Ladd 1995, Yu, Bally, & Devine 1997, Wilking et al. 1997, Gómez et al. 1998, Stanke et al. 1998, Phelps & Barsony 1999).

Class 0 objects appear to be short-lived compared to both pre-stellar cores/fragments (see Sect. II above) and Class I near-IR sources. For example, in the ρ Oph main cloud where the IRAM 30 m mapping study of Motte et al. (1998) provides a reasonably complete census of both pre- and proto-stellar condensations down to $\lesssim 0.1 M_{\odot}$, there are only two good Class 0 candidates (including the prototypical object VLA 1623 – AWB93), while there are ~ 15 –30 near-IR Class I sources (e.g. WLY89, AM94, Greene et al. 1994, Barsony & Ressler 1999, Bontemps et al. 1999).

Under the assumption that ρ Oph is representative and forming stars at a roughly constant rate, the lifetime of Class 0 objects should thus be approximately an order of magnitude shorter than the lifetime of Class I sources (see 1. above), i.e., typically ~ 1 –3 $\times 10^4$ yr. The jet-like morphology and short dynamical timescales of Class 0 outflows are consistent with this estimate (e.g. Barsony et al. 1998, see III–D below). A lifetime as short as a few 10^4 yr supports the interpretation of Class 0 objects as very young accreting protostars (see, e.g., Fletcher & Stahler 1994 and Barsony 1994).

Regions like the Serpens, Orion, or Perseus/NGC1333 complexes seem to be particularly rich in Class 0 objects, and this is probably indicative of fairly high levels of ongoing, likely induced star formation activity (e.g. Hurt & Barsony 1996, Chini et al. 1997b, Yu et al. 1997, Barsony et al. 1998). For instance, we estimate the current star formation rate in Orion-OMC-3 to be $\sim 2 \times 10^{-3} M_{\odot} \text{ yr}^{-1}$, which is 1–2 orders of magnitude larger than the star formation rates characterizing the Trapezium, NGC 1333, and IC 348 near-IR clusters when averaged over $\gtrsim 10^6$ yr periods (see Lada, Alves, & Lada 1996).

B. Density Structure of the Protostellar Environment

1. *Envelope.* In contrast to *pre-stellar* cores, the envelopes of low-mass Class 0 and Class I *protostars* are always found to be strongly centrally-condensed and do *not* exhibit any inner flattening in their (sub)millimeter continuum radial intensity profiles. In practice, this means that, when protostars are mapped with the resolution of the largest single-dish telescopes, the measured peak flux density is typically a fraction $\gtrsim 20\%$ of the flux integrated over five beam widths. For comparison, the same fraction is $\lesssim 10\%$ for pre-stellar cores. (Sub)millimeter continuum maps indicate that protostellar envelopes in regions of isolated star formation such as Taurus have radial density gradients generally consistent with $\rho(r) \propto r^{-p}$ with $p \sim 1.5$ –2 over more than ~ 10000 –15000 AU in radius (e.g. Walker, Adams, & Lada 1990, Ladd et al. 1991, Motte 1998, Motte et al. 1999, see also Mundy et

al. this volume). The estimated density gradient thus agrees with most collapse models which predict a value of p between 1.5 and 2 during the protostellar accretion phase (e.g. Whitworth & Summers 1985). Some studies have, however, inferred shallower density gradients ($p \sim 0.5$ –1 – e.g. Barsony & Chandler 1993, Chandler, Barsony, & Moore 1998). In any case, the densities and masses measured for the envelopes around the bona-fide Class I objects of Taurus appear to be consistent within a factor of ~ 4 with the predictions of the “standard” inside-out collapse theory (e.g. Shu et al. 1993) for $\sim 10^5$ yr-old, isolated protostars (Motte 1998, Motte et al. 1999).

The situation is markedly different in star-forming clusters. In ρ Ophiuchi in particular, the circumstellar envelopes of Class I and Class 0 protostars are observed to be very compact: they merge with dense cores, other envelopes, and/or the diffuse ambient cloud at a *finite* radius $R_{out} \lesssim 5000$ AU (Motte et al. 1998). This is $\gtrsim 3$ times smaller than the collapse expansion wavefront at a ‘Class I age’ of $\sim 2 \times 10^5$ yr in the standard theory of isolated protostars, emphasizing the fact that each YSO has a finite ‘sphere of influence’ in ρ Oph. Similar results were obtained in the case of the Perseus Class 0 sources NGC1333-4A, NGC1333-2, L1448-C, and L1448-N (e.g. Motte 1998). Moreover, the envelopes of these Perseus protostars are 3 to 10 times denser than the singular isothermal sphere for a sound speed $a = 0.2$ km s $^{-1}$. This suggests that, prior to collapse, the main support against gravity was turbulent and/or magnetic in origin rather than purely thermal (see also Mardones et al. 1997).

2. Disks and multiplicity. Many Class 0 protostars are in fact multiple systems, when viewed at sub-arcsecond resolution, sharing a common envelope and sometimes a circumbinary disk (e.g. Looney et al. 1999 – see also col. 11 of Table 1 and chapter by Mundy, Looney, & Welch). These protobinaries probably formed by dynamical fragmentation during (or at the end of) the isothermal collapse phase (e.g. Chapman et al. 1992, Bonnell 1994, Boss & Myhill 1995). Interestingly enough, only cores with inner density profiles as flat as $\rho \propto r^{-1}$ or flatter (like observed pre-stellar cores – see Sect. II), can apparently fragment during collapse (Myhill & Kaula 1992, Boss 1995, Burkert et al. 1997).

Despite the difficulty of discriminating between the disk and envelope components, existing (sub)millimeter continuum interferometric measurements suggest that the “disks” of Class 0 objects are a factor of $\gtrsim 10$ less massive than their surrounding circumstellar envelopes (e.g. Chandler et al. 1995, Pudritz et al. 1996, Looney et al. 1999, Hogerheijde 1998, Motte 1998, Wilner & Lay this volume).

C. Direct Evidence for Infall

Rather convincing spectroscopic signatures of gravitational infall have been reported toward several Class 0 objects, confirming their protostellar nature (e.g. Walker et al. 1986, Zhou et al. 1993, Gregersen et al. 1997, Mardones et al. 1997, see also col. 10 of Table 1). Inward motions can be traced by optically thick molecular lines which should (locally) exhibit asymmetric self-absorbed profiles skewed to the blue (see Myers, Evans, & Ohashi, this volume). The interpretation is often complicated by the simultaneous presence of rotation and/or outflow (e.g. Menten et al. 1987, Walker et al. 1994, Cabrit et al. 1996).

A comprehensive survey of a sample of 47 embedded YSOs in $\text{H}_2\text{CO}(2_{12}-1_{11})$ and $\text{CS}(2-1)$ suggests that infall is more prominent in Class 0 than in Class I sources (Mardones et al. 1997): In these transitions, infall asymmetries are detected toward 40–50 % of Class 0 objects but less than 10 % of Class I sources. This is qualitatively consistent with a decline of infall/accretion rate with evolutionary stage (see III–D below). However, a more recent survey by Gregersen et al. (1999) using $\text{HCO}^+(3-2)$ finds no difference in the fraction of sources with “blue profiles” between Class 0 and Class I sources. The $\text{HCO}^+(3-2)$ line is more optically thick than $\text{H}_2\text{CO}(2_{12}-1_{11})$ and $\text{CS}(2-1)$, hence a better tracer of infall at advanced stages. This result shows that some infall is still present at the Class I stage but remains consistent with a decline of the net accretion rate with time. The outflow is so broad in Class I sources that there often appears to be little transfer of mass to the inner ~ 2000 AU radius region around these objects (e.g. Fuller et al. 1995b, Cabrit et al. 1996, Brown & Chandler 1999).

D. Decline of Outflow and Inflow with Time

1. Evolution from Class 0 to Class I. Most, if not all, Class 0 protostars drive powerful, “jet-like” CO molecular outflows (see, e.g., Bachiller 1996 and Richer et al., this volume, for reviews). The mechanical luminosities of these outflows are often of the same order as the bolometric luminosities of the central sources (e.g. Curiel et al. 1990, AWB93, Barsony et al. 1998). In contrast, while there is good evidence that some outflow activity exists throughout the accretion phase (e.g. Terebey et al. 1989, Parker et al. 1991, Bontemps et al. 1996a), the CO outflows from Class I sources tend to be much less powerful and less collimated than those from Class 0 objects.

In an effort to quantify the evolution of mass loss during the protostellar phase, Bontemps et al. (1996a – hereafter BATC) obtained and analyzed a homogeneous set of $\text{CO}(2-1)$ outflow data around a large sample of low-luminosity ($L_{bol} < 50 L_{\odot}$), nearby ($d < 450$ pc) self-embedded YSOs. Their results show that Class 0 objects lie an order of magnitude above the well-known (e.g. Cabrit & Bertout 1992) correlation between outflow momentum flux (F_{CO}) and bolometric lu-

minosity (L_{bol}) holding for Class I sources (see $F_{\text{CO}} - L_{\text{bol}}$ diagram shown in Fig. 5 of BATC). Furthermore, BATC found that F_{CO} was well correlated with M_{env} in their *entire* sample (including both Class I and Class 0 sources). The same correlation was noted independently on other source samples by Moriarty-Schieven et al. (1994), Hogerheijde et al. (1998), and Henning & Launhardt (1998). As argued by BATC, this new correlation is independent of the $F_{\text{CO}} - L_{\text{bol}}$ correlation and most likely results from a progressive decrease of outflow power with time during the accretion phase. This is illustrated in the normalized $F_{\text{CO}} c/L_{\text{bol}}$ versus $M_{\text{env}}/L_{\text{bol}}^{0.6}$ diagram of Fig. 8, which should be essentially free of any luminosity effect.

Since magneto-centrifugal accretion/ejection models of bipolar outflows (e.g. Shu et al. 1994, Ferreira & Pelletier 1995, Fiege & Henriksen 1996, Ouyed & Pudritz 1997) predict a direct proportionality between accretion and ejection, BATC proposed that the decline of outflow power with evolutionary stage seen in Fig. 8 reflects a corresponding decrease in the mass-accretion/infall rate. The results of BATC indicate that \dot{M}_{jet} declines from $\sim 10^{-6} M_{\odot} \text{ yr}^{-1}$ for the youngest Class 0 protostars to $\sim 2 \times 10^{-8} M_{\odot} \text{ yr}^{-1}$ for the most evolved Class I sources, suggesting a decrease in \dot{M}_{acc} from $\sim 10^{-5} M_{\odot} \text{ yr}^{-1}$ to $\sim 2 \times 10^{-7} M_{\odot} \text{ yr}^{-1}$ if realistic jet model parameters are adopted ($\dot{M}_{\text{jet}}/\dot{M}_{\text{acc}} \sim 0.1-0.3$, $V_{\text{jet}} \sim 100 \text{ km s}^{-1}$). These indirect estimates of \dot{M}_{acc} for Class 0 and Class I protostars should only be taken as indicative of the true evolutionary trend. Nevertheless, it is interesting to note that they agree well with independent estimates of the rates of envelope dissipation based on circumstellar mass versus age arguments (Ward-Thompson 1996, Ladd, Fuller, & Deane 1998).

As illustrated by the evolutionary tracks of Fig. 7b, a decline of \dot{M}_{acc} with time does not imply a higher accretion luminosity for Class 0 objects compared to Class I sources because the central stellar mass is smaller at the Class 0 stage and the stellar radius is likely to be larger (see Henriksen, André, & Bontemps 1997 – hereafter HAB97).

2. Link with the collapse initial conditions. The apparent decay of \dot{M}_{acc} from the Class 0 to the Class I stage may be linked with the density structure observed for pre-stellar cores/condensations (Sect. II). (Magneto)hydrodynamic collapse models predict a time-dependent accretion history when the radial density profile at the onset of fast protostellar collapse differs from $\rho \propto r^{-2}$ (e.g. Foster & Chevalier 1993 – FC93, Tomisaka 1996, McLaughlin & Pudritz 1997, HAB97, Basu 1997, Safier, McKee, & Stahler 1997, Li 1998, Ciolek & Königl 1998). In particular, when starting from Bonnor-Ebert-like initial conditions resembling observed pre-stellar cores, these studies find that supersonic infall velocities develop prior to the formation of the central hydrostatic protostellar object at $t = 0$ (see, e.g., FC93). Observationally, this

early collapse phase should correspond to ‘isothermal protostars’ (see II–E for possible examples). During the protostellar accretion phase ($t > 0$), because of the significant infall velocities achieved at $t < 0$, \dot{M}_{acc} is initially higher than the standard $\sim a^3/G$ value obtained for the inside-out collapse of a static singular isothermal sphere (Shu 1977, see also Sect. I). The accretion rate then converges toward the standard value of the Shu solution, and declines again below a^3/G at late times if the reservoir of mass is finite. By comparison with the rough estimates of \dot{M}_{acc} given above, it is tempting to identify the short period of energetic accretion ($\dot{M}_{\text{acc}} \sim 10 \times a^3/G$) predicted by the models just after point-mass formation with the observationally-defined Class 0 stage (HAB97, see Fig. 8). In this view, the more evolved Class I objects would correspond to the longer period of moderate accretion/ejection when the accretion rate approaches the standard value ($\dot{M}_{\text{acc}} \lesssim a^3/G \sim 2 \times 10^{-6} \text{ M}_{\odot} \text{ yr}^{-1}$ for a cloud temperature of ~ 10 K). Using simple pressure-free analytical calculations (justified since the inflow becomes supersonic early on), HAB97 could indeed find a good overall fit to the empirical accretion history inferred by BATC on the basis of CO outflow observations (see Fig. 8).

In the absence of magnetic fields, FC93 have shown that the timescale for convergence to the standard accretion rate of Shu (1977) depends on the radius of the flat inner core (R_{flat}) relative to the outer radius of the initial pre-collapse condensation (R_{out}). They found that a phase of constant $\sim a^3/G$ accretion rate is achieved only when $R_{\text{out}}/R_{\text{flat}} \gtrsim 20$, typically after ~ 10 free-fall times of the flat inner region, for a period lasting ~ 15 free-fall times when $R_{\text{out}}/R_{\text{flat}} = 20$ and progressively longer as $R_{\text{out}}/R_{\text{flat}}$ increases. Since observations suggest $R_{\text{out}}/R_{\text{flat}} \lesssim 3$ in Ophiuchus and $R_{\text{out}}/R_{\text{flat}} \gtrsim 15$ in Taurus (see II–C, III–B, and Motte et al. 1998), one may expect a marked time-dependence of \dot{M}_{acc} in Ophiuchus but a reasonable agreement with the constant accretion rate of the self-similar theory of Shu et al. (1987, 1993) in Taurus. Indeed, HAB97 note that there is a much better continuity between Class 0 and Class I protostars in Taurus than in Ophiuchus (see also André 1997).

Finally, we stress that the absolute values of \dot{M}_{acc} in the Class 0 and Class I stages are presently quite uncertain. An alternative interpretation of the evolution seen in Fig. 8 is that Class 0 protostars accrete at a rate roughly consistent with $\sim a^3/G$, while most Class I sources are in a terminal accretion phase with $\dot{M}_{\text{acc}} \lesssim 0.1 \times a^3/G$, resulting from the finite effective reservoir of mass available to each object in clusters (e.g. Motte et al. 1998 and III–B) and/or from the effects of outflows dispersing the envelope (e.g. Myers et al. 1998, Ladd et al. 1998). Distinguishing between this possibility and that advocated above will require direct measurements of the mass accretion rates.

IV. CONCLUSIONS AND IMPLICATIONS

The observational studies discussed in Sect. II demonstrate that pre-stellar cores/fragments are characterized by flat inner radial density gradients. This, in turn, suggests the initial conditions for fast protostellar collapse are non-singular, i.e., the density profile at the onset of collapse is not infinitely centrally condensed. (Sub)millimeter observations also set strong constraints on protostellar evolution (Sect. III). The fact that young (Class 0) protostars drive more powerful outflows than evolved (Class I) protostars suggests that the mass accretion rate \dot{M}_{acc} decreases by typically a factor of ~ 5 –10 from the Class 0 to the Class I stage (III–D). Such a decline in \dot{M}_{acc} during the protostellar accretion phase may be the direct result of a flattened initial density profile (see III–D). Based on these observational constraints, we suggest that most protostars form in a dynamical rather than quasi-static fashion.

The results summarized in this chapter also have broader implications concerning, e.g., the origin of the IMF. As pointed out in Sect. II–E, the pre-stellar condensations observed in regions of multiple star formation such as ρ Ophiuchi are finite-size structures, typically a few 1000 AU in radius, which are clearly not scale-free. This favors a picture of star formation in clusters in which individual protostellar collapse is initiated in compact dense clumps resulting from fragmentation and resembling more finite-size Bonnor-Ebert cloudlets than singular isothermal spheres. Such condensations may correspond to dense, low-ionization pockets decoupling themselves from the parent molecular cloud as a result of ambipolar diffusion and/or the dissipation of turbulence (e.g. Mouschovias 1991, Myers 1998, Nakano 1998). They would thus be free to undergo Jeans-like gravitational instabilities and collapse under the influence of external disturbances, of which there are many types in regions of multiple star formation (e.g. Pringle 1989, Whitworth et al. 1996, Motte et al. 1998, Barsony et al. 1998). By contrast, the low-density regions of the ambient cloud, being more ionized, would remain supported against collapse by static and/or turbulent magnetic fields. The typical separation between individual condensations should be of order the Jeans length in the parent cloud/core, in rough agreement with observations (e.g. Motte et al. 1998).

In this observationally-driven scenario of fragmentation and collapse, stars are built from bounded fragments which represent finite reservoirs of mass. The star formation efficiency within these fragments is high: most of their ‘initial’ masses at the onset of collapse end up in stars. If this is true, it implies that the physical mechanisms responsible for the formation of pre-stellar cores/condensations in molecular clouds, such as turbulent fragmentation (e.g. Padoan, Nordlund, & Jones 1997), play a key role in determining the IMF of embedded clusters. Such a picture, which we favor for regions of mul-

tiple star formation, is consistent with some theoretical scenarios of protocluster formation (e.g. Larson 1985, Klessen, Burkert, & Bate 1998). It need not be universal, however, and is in fact unlikely to apply to regions of isolated star formation like the Taurus cloud. In these regions, protostars may accrete from larger reservoirs of mass, and feed-back processes such as stellar winds may be more important in limiting accretion and defining stellar masses (e.g. Shu et al. 1987, Silk 1995, Adams & Fatuzzo 1996, Velusamy & Langer 1998).

With the advent of major new facilities at far-IR and submillimeter wavelengths, the next decade promises to be at least as rich in observational discoveries as the past ten years. By combining the capabilities of space telescopes such as FIRST with those of large ground-based arrays such as the LSA/MMA, it will be possible to study the detailed physics of complete samples of young protostars and pre-collapse fragments, in a variety of star-forming clouds, and down to the brown-dwarf mass regime. This should tremendously improve our global understanding of the initial stages of star formation in the Galaxy.

Acknowledgements. We thank C. Correia for providing unpublished data shown in Fig. 2, G. Ciolek for Fig. 3b, P. Myers for Fig. 7a, and N. Grosso for assistance in preparing some of the figures. We are also grateful to F. Motte and the referee, N. Evans, for useful comments and suggestions.

REFERENCES

- Abergel, A., Bernard, J.P., Boulanger, F. et al. 1996. ISOCAM mapping of the ρ Ophiuchi main cloud. *Astron. Astrophys.* 315:L329–L332
- Abergel, A., Bernard, J.P., Boulanger, F. et al. 1998. The dense core Oph D seen in extinction by ISOCAM. In *Star Formation with ISO*, eds. J.L. Yun & R. Liseau, *A.S.P. Conf. Series*, 132:220–229
- Adams F.C., and Fatuzzo, M. 1996. A theory of the initial mass function for star formation in molecular clouds. *Astrophys. J.*, 464:256–271
- Adams F.C., Lada C.J., and Shu, F.H. 1987. Spectral evolution of young stellar objects. *Astrophys. J.* 312:788–806
- Akeson, R.L., and Carlstrom, J.E. 1997. Magnetic field structure in protostellar envelopes. *Astrophys. J.* 491:254–266
- André, P. 1997. The evolution of flows and protostars. In *Herbig-Haro Flows and the Birth of Low Mass Stars. Proc. IAU Symp. 182*, eds. B. Reipurth and C. Bertout (Dordrecht: Kluwer), pp. 483–494.
- André, P., and Montmerle, T. 1994. From T Tauri stars to protostars: Circumstellar material and young stellar objects in the ρ Ophiuchi cloud. *Astrophys. J.* 420:837–862 (AM94)
- André, P., Motte, F., and Bacmann, A. 1999. Discovery of an extremely young accreting protostar in Taurus. *Astrophys. J. Lett.*, in press
- André P., Ward-Thompson D., and Barsony, M. 1993. Submillimeter continuum observations of ρ Ophiuchi A: The candidate protostar VLA 1623 and prestellar clumps. *Astrophys. J.* 406:122–141 (AWB93)
- André P., Ward-Thompson D., and Motte, F. 1996. Probing the initial conditions of star formation: the structure of the prestellar core L1689B. *Astron. Astrophys.* 314:625–635
- André, P., Martín-Pintado, J., Despois, D., and Montmerle T. 1990. Discovery of a remarkable bipolar flow and exciting source in the ρ Ophiuchi cloud core. *Astron. Astrophys.* 236:180–192
- Anglada, G., Estalella, R., Rodríguez, L.F., Torrelles, J.M., López, R., & Cantó, J. 1991. A double radio source at the center of the outflow in L723. *Astrophys. J.* 376:615–617
- Anglada, G., Rodríguez, L.F., Cantó, J., Estalella, R., & Torrelles, J.M. 1992. Radio continuum from the powering sources of the RNO 43, HARO 4-255 FIR, B335, and PV Cephei outflows and from the

- Herbig-Haro object 32A. *Astrophys. J.* 395:494–500
- Avery, L.W., Hayashi, S.S., and White, G.J. 1990. The unusual morphology of the high-velocity gas in L723 - One outflow or two? *Astrophys. J.* 357:524–530
- Bachiller, R. 1996. Bipolar molecular outflows from young stars and protostars. *Ann. Rev. Astron. Astrophys.* 34:111–154
- Bachiller, R., André, P., and Cabrit, S. 1991a. Detection of the exciting source of the spectacular molecular outflow L1448 at $\lambda\lambda$ 1-3 mm. *Astron. Astrophys.* 241:L43–L46
- Bachiller, R., Martín-Pintado, J., Tafalla, M., Cernicharo, J., Lazareff, B. 1990. High-velocity molecular bullets in a fast bipolar outflow near L1448/IRS3. *Astron. Astrophys.* 231:174–186
- Bachiller, R., Guilloteau, S., Dutrey, A., Planesas, P., Martín-Pintado, J. 1995. The jet-driven molecular outflow in L 1448. CO and continuum synthesis images. *Astron. Astrophys.* 299:857–868
- Bachiller, R., Guilloteau, S., Gueth, F., Tafalla, M., Dutrey, A., Codella, C., and Catsets, A. 1998. A molecular jet from SVS 13B near HH 7-11. *Astron. Astrophys.* 339:L49–L52
- Bachiller, R., Martín-Pintado, J., & Planesas, P. 1991b. High-velocity molecular jets and bullets from IRAS 03282+3035. *Astron. Astrophys.* 251:639–648
- Bachiller, R., Terebey, S., Jarrett, T., Martín-Pintado, J., Beichman, C.A., & van Buren, D. 1994. Shocked molecular gas around the extremely young source IRAS 03282+3035. *Astrophys. J.* 437:296–304
- Bacmann, A., André, P., Abergel, A. et al. 1997. An ISOCAM absorption study of dense cloud cores. In *Star Formation with ISO*, eds. J.L. Yun & R. Liseau, *A.S.P. Conf. Series*, 132:307–313
- Bally, J., Lada, E.A., & Lane, A.P. 1993. The L1448 Molecular Jet. *Astrophys. J.* 418:322–327
- Balsara D., Ward-Thompson D., Pouquet A., Crutcher R. M. 1998. An MHD model of the inter-stellar medium and a new method of accretion onto dense star-forming cores. In *Interstellar Turbulence*, eds. J. Franco and A. Carraminana A., (Cambridge: University Press), pp. 49–
- Barsony, M. 1994. Class 0 protostars. In *Clouds, Cores, and Low-mass Stars*, eds. D. P. Clemens and R. Barvainis, *A.S.P. Conf. Series*, 65:197–206
- Barsony, M., and Chandler, C. J. 1992. On the origin of submillimeter emission from young stars in Taurus-Auriga. *Astrophys. J.* 384:L53–L57
- Barsony, M., and Chandler, C. J. 1993. The circumstellar density distribution of L1551NE. *Astrophys. J.* 406:L71–L74
- Barsony, M., Ressler, M. 1999. The initial luminosity function for L1688: New mid-IR imaging photometry. *Astrophys. J.*, in prepa-

ration

- Barsony, M., Ward-Thompson, D., André, P., and O'Linger, J. 1998. Protostars in Perseus: Outflow induced fragmentation. *Astrophys. J.* 509:733–748
- Basu, S. 1997. A Semianalytic Model for Supercritical Core Collapse: Self-similar Evolution and the Approach to Protostar Formation. *Astrophys. J.* 485:240–253
- Basu, S., and Mouschovias, T.Ch. 1995. Magnetic Braking, Ambipolar Diffusion, and the Formation of Cloud Cores and Protostars. III. Effect of the Initial Mass-to-Flux Ratio. *Astrophys. J.* 453:271–283
- Bate, M.R. 1998. Collapse of a Molecular Cloud Core to Stellar Densities: The First Three-dimensional Calculations. *Astrophys. J. Lett.* 508:L95–L98
- Beckwith, S.V.W., Sargent A.I, Chini, R.S., Guesten, R. 1990. A survey for circumstellar disks around young stellar objects. *Astron. J.* 99:924–945
- Beichman, C.A., Myers, P.C., Emerson, J.P. et al. 1986. Candidate solar-type protostars in nearby molecular cloud cores. *Astrophys. J.* 307:337–349
- Bence, S.J., Richer, J.S., and Padman, R. 1996. RNO 43: a jet-driven super-outflow. *Mon. Not. Roy. Astron. Soc.* 279:866–883
- Benson, P. J., and Myers, P. C. 1989. A survey for dense cores in dark clouds. *Astrophys. J. Sup.* 71:89–108
- Beichman, C.A., Myers, P.C., Emerson, J.P. et al. 1986. Candidate solar-type protostars in nearby molecular cloud cores. *Astrophys. J.* 307:337–349
- Blake, G.A., Sandell, G., van Dishoek, E.W., Groesbeck, T.D., Mundy, L.G., and Aspin, C. 1995. A molecular line study of NGC 1333/IRAS 4. *Astrophys. J.* 441:689–701
- Blitz, L. 1993. Giant molecular clouds. In *Protostars & Planets III*, eds. E. H. Levy and J. I. Lunine (Tucson: Univ. of Arizona Press), pp. 125–161.
- Blottiau, P., Chièze, J.P., and Bouquet, S. 1988. An asymptotic self-similar solution for the gravitational collapse *Astron. Astrophys.* 207:24–36
- Brown, D. W., and Chandler, C.J. 1999. Circumstellar kinematics and the measurement of stellar mass for the protostars TMC1A and TMC1A. *Mon. Not. Roy. Astron. Soc.* April/May
- Bonnell, I. A. 1994. Fragmentation and the formation of binary and multiple systems. In *Clouds, Cores, and Low-mass Stars*, eds. D. P. Clemens and R. Barvainis, *A.S.P. Conf. Series*, 65:115–124
- Bonnell, I. A., Bate, M. R., Clarke, C. J. and Pringle, J.E. 1997. Accretion and the stellar mass spectrum in small clusters. *Mon. Not. Roy. Astron. Soc.* 285:201–208
- Bontemps, S. 1996. Evolution de l'éjection de matière des proto-étoiles.

Ph. D. Dissertation, University of Paris XI

- Bontemps, S., André, P., and Ward-Thompson, D. 1995. Deep VLA search for the youngest protostars: A Class 0 source in the HH24-26 region. *Astron. Astrophys.* 297:98–102
- Bontemps, S., André, P., Terebey, S., and Cabrit, S. 1996a. Evolution of outflow activity around low-mass embedded young stellar objects. *Astron. Astrophys.* 311:858–872 (BATC)
- Bontemps, S., Nordh, L., Olofsson, G. et al. 1999. An ISOCAM Deep Census of Low-Mass Stars in ρ Ophiuchi – Mass Function in a Young Embedded Cluster. In *The Universe as seen by ISO*, eds. P. Cox and M. Kessler (Noordwijk: ESA-SP), in press
- Bontemps, S., Ward-Thompson, D., and André, P. 1996b. Discovery of a jet emanating from the protostar HH 24 MMS. *Astron. Astrophys.* 314:477–483
- Boss, A.P. 1995. Gravitational Collapse and Binary Protostars. *Rev. Mex. A. A. (ser. de conf.)* 1:165–177
- Boss, A.P., & Myhill, E.A. 1995. Collapse and Fragmentation of Molecular Cloud Cores. III Initial Differential Rotation. *Astrophys. J.* 451:218–224
- Boss, A.P., & Yorke, H.W. 1995. Spectral energy of first protostellar cores: Detecting 'class -I' protostars with ISO and SIRTIF. *Astrophys. J.* 439:L55–L58
- Bourke, T.L., Hyland, A.R., & Robinson, G. 1995a. Studies of star formation in isolated small dark clouds - I. A catalogue of southern Bok globules: optical and IRAS properties. *Mon. Not. Roy. Astron. Soc.* 276:1052-1066
- Bourke, T.L., Hyland, A.R., & Robinson, G. 1995b. Studies of star formation in isolated small dark clouds - II. A southern ammonia survey. *Mon. Not. Roy. Astron. Soc.* 276:1067-1084
- Bourke, T. L., Garay, G., Lehtinen, K. K., et al. 1997. Discovery of a Highly Collimated Molecular Outflow in the Southern Bok Globule BHR 71. *Astrophys. J.* 476:781–800
- Brown, D.W., and Chandler, C.J. 1999. Circumstellar kinematics and the measurement of stellar mass for the protostars TMC1 and TMC1A. *Mon. Not. Roy. Astron. Soc.* April/May
- Burkert, A., Bate, M.R., and Bodenheimer, P. 1997. Protostellar fragmentation in a power-law density distribution. *Mon. Not. Roy. Astron. Soc.* 289:497-504
- Butner, H.M., Lada, E.A., and Loren, R.B. 1995. Physical Properties of Dense Cores: DCO + Observations. *Astrophys. J.* 448:207–225
- Cabrit, S., & André, P. 1991. An observational connection between circumstellar disk mass and molecular outflows. *Astrophys. J. Lett.* 379:L25–L28
- Cabrit S., & Bertout C. 1992. CO line formation in bipolar flows. III - The energetics of molecular flows and ionized winds. *Astron.*

- Astrophys.* 261:274–284
- Cabrit S., Goldsmith, P.F., and Snell, R.L. 1988. Identification of RNO 43 and B335 as two highly collimated bipolar flows oriented nearly in the plane of the sky. *Astrophys. J.* 334:196–208
- Cabrit, S., Guilloteau, S., André, P., Bertout, C., Montmerle, T., & Schuster, K. 1996. Plateau de Bure observations of HL Tauri: outflow motions in a remnant circumstellar envelope. *Astron. Astrophys.* 305:527–540
- Casali, M. M., Eiroa, C., and Duncan, W. D. 1993. A second phase of star formation in the Serpens core. *Astron. Astrophys.* 275:195–200
- Ceccarelli, C., Caux, E., White, G. J. et al. 1998. The far infrared line spectrum of the protostar IRAS 16293-2422. *Astron. Astrophys.* 331:372–382
- Cernicharo, J., Lefloch, B., Cox, P. et al. 1998. Induced Massive Star Formation in the Trifid Nebula? *Science* 282:462–465
- Chandler, C.J., Barsony, M., and Moore, T.J.T. 1998. The circumstellar envelopes around three protostars in Taurus. *Mon. Not. Roy. Astron. Soc.* 299:789–798
- Chandler, C.J., Gear, W.K., Sandell, G., Hayashi, S., Duncan, W.D., & Griffin, M.J. 1990. B335 - Protostar or embedded pre-main-sequence star? *Mon. Not. Roy. Astron. Soc.* 243:330–335
- Chandler, C.J., Koerner, D.W., Sargent, A.I., & Wood, D.O.S. 1995. Dust Emission from Protostars: The Disk and Envelope of HH 24 MMS. *Astrophys. J.* 449:L139–L142
- Chapman, S.J., Davies, J.R., Disney, M.J., Nelson, A.H., Pongracic, H., Turner, J.A., Whitworth, A.P. 1992. The formation of binary and multiple star systems. *Nature* 359:207–210
- Chen, H., Grenfell, T. G., Myers, P. C., and Hughes, J. D. 1997. Comparison of Star Formation in Five Nearby Molecular Clouds. *Astrophys. J.* 478:295–312
- Chen, H., Myers, P. C., Ladd, E F., and Wood, D.O.S. 1995. Bolometric temperature and young stars in the Taurus and Ophiuchus complexes. *Astrophys. J.* 445:377–392
- Chièze, J.-P., and Pineau des Forêts, G. 1987. The fragmentation of molecular clouds. II - Gravitational stability of low-mass molecular cloud cores. *Astron. Astrophys.* 183:98–108
- Chini, R., Krügel, E., Haslam, C.G.T., Kreysa, E., Lemke, R., Reipurth, B., Sievers, A., & Ward-Thompson, D. 1993. Discovery of a cold and gravitationally unstable cloud fragment. *Astron. Astrophys.* 272:L5–L8
- Chini, R., Reipurth, B., Sievers, A., Ward-Thompson, D., Haslam, C.G.T., Kreysa, E., Lemke, R. 1997a. Cold dust around Herbig-Haro energy sources: morphology and new protostellar candidates. *Astron. Astrophys.* 325:542–550

- Chini, R., Reipurth, B., Ward-Thompson, D., Bally, J., Nyman, L.A., Sievers, A., & Billawala, Y. 1997b. Dust Filaments and Star Formation in OMC-2 and OMC-3. *Astrophys. J.* 474:L135–L138
- Ciolek, G.E., & Königl, A. 1998. Dynamical Collapse of Nonrotating Magnetic Molecular Cloud Cores: Evolution through Point-Mass Formation. *Astrophys. J.* 504:257–279
- Ciolek, G.E., & Mouschovias, T.Ch. 1994. Ambipolar diffusion, interstellar dust, and the formation of cloud cores and protostars. III: Typical axisymmetric solutions. *Astrophys. J.* 425:142–160
- Clemens, D. P., and Barvainis, R. 1988. A catalog of small, optically selected molecular clouds - Optical, infrared, and millimeter properties. *Astrophys. J. Sup.* 68:257–286
- Curiel, S., Raymond, J.C., Rodríguez, L.F., Cantó, J., & Moran, J.M. 1990. The exciting source of the bipolar outflow in L1448. *Astrophys. J. Lett.* 365:L85–L88
- Curiel, S., Rodríguez, L.F., Moran, J.M., and Cantó, J. 1993. The triple radio continuum source in Serpens - The birth of a Herbig-Haro system? *Astrophys. J.* 415:191–203
- Davidson, J.A. 1987. Low-Luminosity embedded sources and their environs. *Astrophys. J.* 315:602–620
- Davis, C.J., and Eisloffel, J. 1995. Near-infrared imaging in H₂ of molecular (CO) outflows from young stars. *Astron. Astrophys.* 300:851–869
- Dent, W.R.F., Matthews, H.E., and Walther, D.M. 1995. CO and shocked H₂ in the highly collimated outflow from VLA 1623. *Mon. Not. Roy. Astron. Soc.* 277:193–209
- Dent, W.R.F., Matthews, H.E., and Ward-Thompson, D. 1998. The submillimetre colour of young stellar objects. *Mon. Not. Roy. Astron. Soc.* 301:1049–1063
- Efstathiou, A., and Rowan-Robinson, M. 1991. Radiative transfer in axisymmetric dust clouds. II - Models of rotating protostars. *Mon. Not. Roy. Astron. Soc.* 252:528–534
- Eiroa, C., Miranda, L.F., Anglada, G., Estalella, R., & Torrelles, J.M. 1994. Herbig-Haro objects associated with extremely young sources in L1527 and L1448. *Astron. Astrophys.* 283:973–977
- Falgarone, E., & Puget, J.-L. 1985. A model of clumped molecular clouds. I - Hydrostatic structure of dense cores. *Astron. Astrophys.* 142:157–170
- Ferreira J., & Pelletier G. 1995. Magnetized accretion-ejection structures. III. Stellar and extragalactic jets as weakly dissipative disk outflows. *Astron. Astrophys.* 295:807–832
- Fiege, J.D., & Henriksen, R.N. 1996. A global model of protostellar bipolar outflow - I. *Mon. Not. Roy. Astron. Soc.* 281:1038–1054
- Fletcher, A. B., and Stahler, S. W. 1994. The luminosity functions of embedded stellar clusters. I: Method of solution and analytic

- results. *Astrophys. J.* 435:313–328
- Foster, P. N., and Chevalier, R. A. 1993. Gravitational Collapse of an Isothermal Sphere. *Astrophys. J.* 416:303–311 (FC93)
- Fuller, G.A., Lada, E.A., Masson, C.R., Myers, P.C. 1995a. The Infrared Nebula and Outflow in Lynds 483. *Astrophys. J.* 453:754–760
- Fuller, G.A., Lada, E.A., Masson, C.R., Myers, P.C. 1995b. The Circumstellar Molecular Core around L1551 IRS 5. *Astrophys. J.* 454:862–871
- Gammie, C.F., and Ostriker, E.C. 1996. Can Nonlinear Hydromagnetic Waves Support a Self-gravitating Cloud? *Astrophys. J.* 466:814–830
- Gibb, A.G. 1999. A VLA search for embedded young stellar objects and protostellar candidates in L1630. *Mon. Not. Roy. Astron. Soc.* in press
- Gibb, A.G., & Davis, C.J. 1998. The outflow from the class 0 protostar HH25MMS: methanol enhancement in a well-collimated outflow. *Mon. Not. Roy. Astron. Soc.* 298:644–656
- Gómez, J.F., Curiel, S., Torrelles, J.M., Rodríguez, L.F., Anglada, G., and Girart, J.M. 1994. The molecular core and the powering source of the bipolar molecular outflow in NGC 2264G. *Astrophys. J.* 436:749–753
- Gómez, M., Hartmann, L., Kenyon, S.J., and Hewett, R. 1993. On the spatial distribution of pre-main-sequence stars in Taurus. *Astron. J.* 105:1927–1937
- Gómez, M., Whitney, B.A., and Wood, K. 1998. A Survey of Optical Jets and Herbig-Haro Objects in the rho Ophiuchi Cloud Core. *Astron. J.* 115:2018–2027
- Greaves, J.S., and Holland, W.S. 1998. Twisted magnetic field lines around protostars. *Astron. Astrophys.* 333:L23–L26
- Greaves, J.S., Holland, W.S., and Ward-Thompson, D. 1997. Submillimeter Polarimetry of Class 0 Protostars: Constraints on Magnetized Outflow Models. *Astrophys. J.* 480:255–261
- Greene, T. P., and Lada C. J. 1996. Near-Infrared Spectra and the Evolutionary Status of Young Stellar Objects: Results of a 1.1–2.4 μm Survey. *Astron. J.* 112:2184–2221
- Greene, T. P., Wilking B. A., André P., Young E. T., and Lada C. J. 1994. Further mid-infrared study of the rho Ophiuchi cloud young stellar population: Luminosities and masses of pre-main-sequence stars. *Astrophys. J.* 434:614–626
- Gregersen, E. M., Evans II, N. J., Mardones, D., and Myers, P.C. 1999. Does Infall End Before the Class I stage? *Astrophys. J.* in press
- Gregersen, E. M., Evans II, N. J., Zhou, S., and Choi, M. 1997. New Protostellar Collapse Candidates: An HCO + Survey of the Class 0 Sources. *Astrophys. J.* 484:256–276

- Grossman, E. N., Masson, C.R., Sargent, A.I., Scoville, N.Z., Scott, S., and Woody, D.P. 1987. A possible protostar near HH 7-11. *Astrophys. J.* 320:356–363
- Gueth, F., Guilloteau, S., Dutrey, A., and Bachiller, R. 1997. Structure and kinematics of a protostar: mm-interferometry of L 1157. *Astron. Astrophys.* 323:943–952
- Güsten, R. 1994. Protostellar condensations. In *The Cold Universe*, eds. T. Montmerle, C.J. Lada, I.F. Mirabel, and J. Trân Thanh Vân, (Gif-sur-Yvette: Editions Frontières), pp. 169–177
- Henning, Th., and Launhardt, R. 1998. Millimetre study of star formation in southern globules. *Astron. Astrophys.* 338:223–242
- Henning, Th., Michel, B., & Stognienko, R. 1995. Dust opacities in dense regions. *Planet. Space Sci.* 43:1333–1343
- Henriksen, R.N., André, P., and Bontemps, S. 1997. Time-dependent accretion and ejection implied by pre-stellar density profiles. *Astron. Astrophys.* 323:549–565 (HAB97)
- Herbst, T.M., Beckwith, S., and Robberto, M. 1997. A New Molecular Hydrogen Outflow in Serpens. *Astrophys. J. Lett.* 486:L59–L62
- Hildebrand, R.H. 1983. The determination of cloud masses and dust characteristics from submillimetre thermal emission. *Quart. J. Roy. Astron. Soc.* 24:267–282
- Hirano, N., Kameya, O., Kasuga, T., and Umemoto, T. 1992. Bipolar outflow in B335 - The small-scale structure. *Astrophys. J. Lett.* 390:L85–L88
- Hodapp, K.-W., and Ladd, E. F. 1995. Bipolar Jets from Extremely Young Stars Observed in Molecular Hydrogen Emission. *Astrophys. J.* 453:715–720
- Hogerheijde, M. R. 1998. The molecular environment of low-mass protostars. *Ph. D. Dissertation, University of Leiden* (Amsterdam: Thesis Publishers)
- Hogerheijde, M. R., van Dishoeck, E. F., Blake, G. A., and van Langevelde, H. J. 1998. Envelope Structure on 700 AU Scales and the Molecular Outflows of Low-Mass Young Stellar Objects. *Astrophys. J.* 502:315–336
- Hogerheijde, M. R., van Dishoeck, E. F., Salverda, J.M., and Blake, G. A. 1999. Envelope Structure of deeply embedded young stellar objects in the Serpens molecular cloud. *Astrophys. J.* in press
- Holland, W.S., Greaves, J.S., Ward-Thompson, D., and André, P. 1996. The magnetic field structure around protostars. Submillimetre polarimetry of VLA 1623 and S106-IR/FIR. *Astron. Astrophys.* 309:267–274
- Hunter, T.R., Neugebauer, G., Benford, D.J., Matthews, K., Lis, D.C., Serabyn, E., and Phillips, T.G. 1998. G34.24+0.13MM: A Deeply Embedded Proto-B-Star. *Astrophys. J. Lett.* 493:L97–L100
- Hurt, R. L., and Barsony, M. 1996. A Cluster of Class 0 Protostars in

- Serpens: An IRAS HIRES Study. *Astrophys. J. Lett.* 460:L45–L48
- Hurt, R. L., Barsony, M., and Wootten, A. 1996. Potential Protostars in Cloud Cores: H 2CO Observations of Serpens. *Astrophys. J.* 456:686–695
- Jenness, T., Scott, P. F., and Padman, R. 1995. Studies of embedded far-infrared sources in the vicinity of H₂O masers - I. Observations. *Mon. Not. Roy. Astron. Soc.* 276:1024–1040
- Jessop, N., & Ward-Thompson, D. 1999. Star Formation in molecular cloud cores. *Mon. Not. Roy. Astron. Soc.* in prep.
- Johnstone, D., and Bally, J. 1999. JCMT/SCUBA sub-millimeter wavelength imaging of the integral-shaped filament in Orion. *Astrophys. J. Lett.* 510:L49–L53
- Kenyon, S.J. and Hartmann, L 1995. Pre-Main-Sequence Evolution in the Taurus-Auriga Molecular Cloud. *Astrophys. J. Suppl.* 101:117–171
- Kenyon, S. J., Calvet, N., and Hartmann, L. 1993a. The embedded young stars in the Taurus-Auriga molecular cloud. I - Models for spectral energy distributions. *Astrophys. J.* 414:676–694
- Kenyon, S.J., Brown, D.I., Tout, C.A., and Berlind, P. 1998. Optical Spectroscopy of Embedded Young Stars in the Taurus-Auriga Molecular Cloud. *Astron. J.* 115:2491–2591
- Kenyon, S.J., Whitney, B.A., Gomez, M., and Hartmann, L. 1993b. The embedded young stars in the Taurus-Auriga molecular cloud. II - Models for scattered light images. *Astrophys. J.* 414:773–792
- Klessen, R.S., Burkert, A., and Bate, M.R. 1998. Fragmentation of Molecular Clouds: The Initial Phase of a Stellar Cluster. *Astrophys. J. Lett.* 501:L205–L208
- Kroupa, P., Tout, C. A., and Gilmore, G. 1993. The distribution of low-mass stars in the Galactic disc. *Mon. Not. Roy. Astron. Soc.* 262:545–587
- Lada, C.J. 1987. Star formation - From OB associations to protostars. In *Star Forming Regions Proc. IAU Symp. 115*, eds. M. Peimbert and J. Jugaku (Dordrecht: Reidel), pp. 1–18.
- Lada, C.J., and Fich, M. 1996. The Structure and Energetics of a Highly Collimated Bipolar Outflow: NGC 2264G. *Astrophys. J.* 459:638–652
- Lada, C.J., and Wilking, B. 1984. The nature of the embedded population in the Rho Ophiuchi dark cloud - Mid-infrared observations. *Astrophys. J.* 287:610–621
- Lada, C.J., Alves, J., and Lada, E. A. 1996. Near-Infrared Imaging of Embedded Clusters: NGC 1333. *Astron. J.* 111:1964–1976
- Ladd, E.F., and Hodapp, K.-W. 1997. A Double Outflow from a Deeply Embedded Source in Cepheus. *Astrophys. J.* 474:749–759
- Ladd, E.F., Adams, F.C., Casey, S., Davidson, J.A., Fuller, G.A., Harper, D.A., Myers, P.C., & Padman, R. 1991. Far-infrared and

- submillimeter wavelength observations of star-forming dense cores. II - Images. *Astrophys. J.* 382:555–569
- Ladd, E.F., Fuller, G.A., and Deane, J.R. 1998. C18O and C17O Observations of Embedded Young Stars in the Taurus Molecular Cloud. I. Integrated Intensities and Column Densities. *Astrophys. J.* 495:871–890
- Langer, W.D., Castets, A., and Lefloch, B. 1996. The IRAS 2 and IRAS 4 Outflows and Star Formation in NGC 1333. *Astrophys. J. Lett.* 471:L111–L114
- Larson, R.B. 1969. Numerical calculations of the dynamics of a collapsing proto-star. *Mon. Not. Roy. Astron. Soc.* 145:271–295
- Larson, R.B. 1985. Cloud fragmentation and stellar masses. *Mon. Not. Roy. Astron. Soc.* 214:379–398
- Launhardt, R. 1996. Dust emission from star-forming regions. IV. Dense cores in the Orion B molecular cloud. *Astron. Astrophys.* 312:569–584
- Launhardt, R., Mezger, P.G., Haslam, C.G.T., Kreysa, E., Lemke, R., Sievers, A., and Zylka, R. 1996. Dust emission from star-forming regions. IV. Dense cores in the Orion B molecular cloud. *Astron. Astrophys.* 312:569–584
- Lay, O. P., Carlstrom, J. E., and Hills, R. E. 1995. NGC 1333 IRAS 4: Further Multiplicity Revealed with the CSO-JCMT Interferometer. *Astrophys. J. Lett.* 452:L73–L76
- Lee, C.W., and Myers, P.C. 1999. A catalogue of optically selected cores. *Astrophys. J. Suppl.* in press
- Lefloch, B., Castets, A., Cernicharo, J., and Loinard, L. 1998. Widespread SiO emission in NGC1333. *Astrophys. J. Lett.* 504:L109–L112
- Lefloch, B., Eislöffel, J., Lazareff, B. 1996. The remarkable Class 0 source Cep E. *Astron. Astrophys.* 313:L17–L20
- Lehtinen, K. 1997. Spectroscopic evidence of mass infall towards an embedded infrared source in the globule DC 303.8-14.2. *Astron. Astrophys.* 317:L5–L8
- Leous, J.A., Feigelson, E.D., André, P., & Montmerle, T. 1991. A rich cluster of radio stars in the Rho Ophiuchi cloud cores. *Astrophys. J.* 379:683–688
- Li, Z.-Y. 1998. Formation and Collapse of Magnetized Spherical Molecular Cloud Cores. *Astrophys. J.* 493:230–246
- Li, Z.-Y., and Shu, F.H. 1996. Magnetized Singular Isothermal Toroids. *Astrophys. J.* 472:211–224
- Li, Z.-Y., and Shu, F.H. 1997. Self-similar Collapse of an Isopedic Isothermal Disk. *Astrophys. J.* 475:237–250
- Looney, L.W., Mundy, L.G., and Welch, W.J. 1999. Unveiling the Envelope and Disk: A sub-arcsecond survey. *Astrophys. J.*
- Lucas, P. W., and Roche P. F. 1997. Butterfly star in Taurus:

- structures of young stellar objects. *Mon. Not. Roy. Astron. Soc.* 286:895–919
- Mardones, D., Myers, P. C., Tafalla, M., Wilner, D. J., Bachiller, R., Garay, G. 1997. A Search for Infall Motions toward Nearby Young Stellar Objects. *Astrophys. J.* 489:719–733
- Mauersberger, R., Wilson, T.L., Mezger, P.G., Gaume, R., Johnston, K.J. 1992. The internal structure of molecular clouds. III - Evidence for molecular depletion in the NGC 2024 condensations. *Astron. Astrophys.* 256:640–651
- McCaughrean, M.J., Rayner, J.T., & Zinnecker, H. 1994. Discovery of a molecular hydrogen jet near IC 348. *Astrophys. J.* 436:L189–L192
- McKee, C.F. 1989. Photoionization-regulated star formation and the structure of molecular clouds. *Astrophys. J.* 345:782–801
- McLaughlin, D.E., and Pudritz, R.E. 1997. Gravitational Collapse and Star Formation in Logotropic and Nonisothermal Spheres *Astrophys. J.* 476:750–765
- McMullin, J.P., Mundy, L.G., Wilking, B.A., Hezel, T., and Blake, G.A. 1994. Structure and chemistry in the northwestern condensation of the Serpens molecular cloud core. *Astrophys. J.* 424:222–236
- Men'shchikov, A.B. & Henning, T. 1997. Radiation transfer in circumstellar disks. *Astron. Astrophys.* 318:879–907
- Menten, K.M., Serabyn, E., Güsten, R., and Wilson, T.L. 1987. Physical conditions in the IRAS 16293-2422 parent cloud. *Astron. Astrophys.* 177:L57–L60
- Mezger, P.G., Sievers, A.W., Haslam, C.G.T., Kreysa, E., Lemke, R., Mauersberger, R., & Wilson, T.L. 1992. Dust emission from star forming regions. II - The NGC 2024 cloud core: Revisited. *Astron. Astrophys.* 256:631–639
- Mizuno, A., Onishi, T., Hayashi, M. et al. 1994. Molecular cloud condensation as a tracer of low-mass star formation. *Nature* 368:719–721
- Molinari, S., Testi, L., Brand, J., Cesaroni, R., and Palla, F. 1998. IRAS 23385+6053: A Prototype Massive Class 0 Object. *Astrophys. J. Lett.* 505:L39–L42
- Moreira, M. C., Yun J. L., Vázquez, R., and Torrelles J. M. 1997. Thermal Radio Sources in Bok Globules. *Astron. J.* 113:1371–1374
- Moriarty-Schieven G.H., Wannier P.G., Keene J., Tamura M. 1994. Circumprotostellar environments. 2: Envelopes, activity, and evolution. *Astrophys. J.* 436:800–806
- Motte, F. 1998. Structure des coeurs denses proto-stellaires: Etude en continuum millimétrique. *Ph. D. Dissertation, University of Paris XI*
- Motte, F., André, P. et al. 1999. Density structure of isolated protostellar envelopes: A millimeter continuum survey of Taurus infrared protostars. *Astron. Astrophys.* in preparation

- Motte, F., André, P., and Neri, R. 1998. The initial conditions of star formation in the ρ Ophiuchi main cloud: wide-field millimeter continuum mapping. *Astron. Astrophys.* 336:150–172
- Mouschovias, T.Ch. 1991. Single-stage fragmentation and a modern theory of star formation. In *The Physics of Star Formation and Early Stellar Evolution*, eds. C. J.Lada & N. D. Kylafis, pp. 449–468
- Mouschovias, T.Ch. 1995. Role of magnetic fields in the early stages of star formation. In *The Physics of the Interstellar Medium and Intergalactic Medium*, eds. A. Ferrara, C.F. Mc Kee, C. Heiles, & P.R. Shapiro (San Francisco: ASP), 80:184–217
- Mundy, L.G., Wootten, H.A., Wilking, B.A., Blake, G.A., & Sargent, A.I. 1992. IRAS 16293 - 2422 - A very young binary system? *Astrophys. J.* 385:306–313
- Mundy, L.G., McMullin, J.P., and Grossman, A.W. 1993. Observations of circumstellar disks at centimeter wavelengths. *Icarus* 106:11–19
- Myers, P.C. 1998. Cluster-forming Molecular Cloud Cores. *Astrophys. J. Lett.* 496:L109–L112
- Myers, P. C., and Benson, P. J. 1983. Dense cores in dark clouds. II. NH_3 observations and star formation. *Astrophys. J.* 266:309–320
- Myers, P. C., and Fuller, G. A. 1993. Gravitational formation times and stellar mass distributions for stars of mass 0.3-30 M_\odot . *Astrophys. J.* 402:635–642
- Myers, P.C., and Ladd, E.F. 1993. Bolometric temperatures of young stellar objects. *Astrophys. J. Lett.* 413:L47–L50
- Myers, P.C., Adams, F.C., Chen, H., and Schaff, E. 1998. Evolution of the Bolometric Temperature and Luminosity of Young Stellar Objects. *Astrophys. J.* 492:703–726
- Myers, P.C., Bachiller, R., Caselli, P., Fuller, G.A., Mardones, D., Tafalla, M., & Wilner, D.J. 1995. Gravitational Infall in the Dense Cores L1527 and L483. *Astrophys. J. Lett.* 449:L65–L68
- Myers, P.C., Fuller, G.A., Mathieu, R.D., Beichman, C.A., Benson, P.J., Schild, R.E., and Emerson, J.P. 1987. Near-infrared and optical observations of IRAS sources in and near dense cores. *Astrophys. J.* 319:340–357
- Myhill, E. A., and Kaula, W. M. 1992. Numerical models for the collapse and fragmentation of centrally condensed molecular cloud cores. *Astrophys. J.* 386:578–586
- Nakano, T. 1984. Contraction of magnetic interstellar clouds. *Fund. Cosm. Phys.* 9:139–231
- Nakano, T. 1998. Star Formation in Magnetic Clouds. *Astrophys. J.* 494:587–604
- Ohashi, N., Hayashi, M., Ho, P.T.P., and Momose, M. 1997. Interferometric Imaging of IRAS 04368+2557 in the L1527 Molecular Cloud Core: A Dynamically Infalling Envelope with Rotation. *Astrophys.*

- J.* 475:211–223
- O’Linger, J., Wolf-Chase, G.A., Barsony, M., and Ward-Thompson, D. 1999. L1448 IRS2: A HIRES-Identified Class 0 Protostar. *Astrophys. J.* in press
- Ossenkopf, V., and Henning, Th. 1994. Dust opacities for protostellar cores. *Astron. Astrophys.* 291:943–959
- Ouyed, R., and Pudritz, R.E. 1997. Numerical Simulations of Astrophysical Jets from Keplerian Disks. I. Stationary Models. *Astrophys. J.* 482:712–732
- Padoan, P., Nordlund, A., & Jones, B.J.T. 1997. *Mon. Not. Roy. Astron. Soc.* 288:145–152
- Palla, F., and Stahler, S.W. 1991. The evolution of intermediate-mass protostars. I - Basic results. *Astrophys. J.* 375:288–299
- Parker, N. D., Padman, R., & Scott, P.F. 1991. Outflows in dark clouds - Their role in protostellar evolution. *Mon. Not. Roy. Astron. Soc.* 252:442–461
- Persi, P., Ferrari-Toniolo, M., Marenzi, A.R., Anglada, G., Chini, R., Krügel, E., and Sepulveda, I. 1994. Infrared images, 1.3 mm continuum and ammonia line observations of IRAS 08076–3556. *Astron. Astrophys.* 282:233–239
- Phelps, R., and Barsony, M. 1999. Herbig-Haro Objects in Serpens & Ophiuchus. *Astron. J.*, in preparation
- Pollack, J.B., Hollenbach, D., Beckwith, S., Simonelli, D.P., Roush, T., Fong, W. 1994. Composition and radiative properties of grains in molecular clouds and accretion disks. *Astrophys. J.* 421:615–639
- Pravdo, S.H., Rodríguez, L.F., Curiel, S., Cantó, J., Torrelles, J.M., Becker, R.H., and Sellgren, K. 1985. Detection of radio continuum emission from Herbig-Haro objects 1 and 2 and from their central exciting source. *Astrophys. J. Lett.* 293:L35–L38
- Preibisch, Th., Ossenkopf, V., Yorke, H.W., & Henning, Th. 1993. The influence of ice-coated grains on protostellar spectra. *Astron. Astrophys.* 279:577–588
- Pringle, J.E. 1989. On the formation of binary stars. *Mon. Not. Roy. Astron. Soc.* 239:361–370
- Pudritz, R.E., Wilson, C.D., Carlstrom, J.E., Lay, O.P., Hills, R.E., and Ward-Thompson, D. 1996. Accretions Disks Around Class 0 Protostars: The Case of VLA 1623. *Astrophys. J. Lett.* 470:L123–L126
- Reipurth, B., Chini, R., Krügel, E., Kreysa, E., and Sievers, A. 1993. Cold dust around Herbig-Haro energy sources: a 1300 μm survey. *Astron. Astrophys.* 273:221–238
- Reipurth, B., Nyman, L.-A., and Chini, R. 1996. Protostellar candidates in southern molecular clouds. *Astron. Astrophys.* 314:258–264
- Richer, J.S., Hills, R.E., & Padman, R. 1992. A fast CO jet in Orion

- B. *Mon. Not. Roy. Astron. Soc.* 254:525–538
- Richer, J.S., Padman, R., Ward-Thompson, D., Hills, R.E., & Harris, A.I. 1993. The molecular environment of S106 IR. *Mon. Not. Roy. Astron. Soc.* 262:839–854
- Ristorcelli, I., Serra, G., Lamarre, J.M. et al. 1998. Discovery of a Cold Extended Condensation in the Orion A Complex. *Astrophys. J.* 496:267–273
- Safier, P.N., McKee, C.F., & Stahler, S.W. 1997. Star Formation in Cold, Spherical, Magnetized Molecular Clouds. *Astrophys. J.* 485:660–679
- Sandell, G. 1994. Secondary calibrators at submillimeter wavelengths. *Mon. Not. Roy. Astron. Soc.* 262:839–854
- Sandell, G., and Weintraub, D.A. 1994. A submillimeter protostar near LkH-alpha 198. *Astron. Astrophys.* 292:L1–L4
- Sandell, G., Aspin, C., Duncan, W.D., Russell, A.P.G., & Robson, E.I. 1991. NGC 1333 IRAS 4 - A very young, low-luminosity binary system. *Astrophys. J.* 376:L17–L20
- Sandell, G., Knee, L.B.G., Aspin, C., Robson, I.E., & Russell, A.P.G. 1994. A molecular jet and bow shock in the low mass protostellar binary NGC 1333-IRAS2. *Astron. Astrophys.* 285:L1–L4
- Sandell, G., Avery, L.W., Baas, F. et al. 1999. A jet-driven, extreme high-velocity outflow powered by a cold, low-luminosity protostar near NGC2023. *Astrophys. J.* in press
- Saraceno, P., André, P., Ceccarelli, C., Griffin, M., and Molinari, S. 1996a. An evolutionary diagram for young stellar objects. *Astron. Astrophys.* 309:827–839
- Saraceno, P., D’Antona, F., Palla, F., Griffin, M., and Tommasi, E. 1996b. The luminosity-mm flux correlation of Class I sources exciting outflows. In *The Role of Dust in the Formation of Stars*, eds. H.U. Käuffel and R. Siebenmorgen (Berlin: Springer), pp. 59–62.
- Scalo, J. 1998. The IMF Revisited: A Case for Variations. In *The Stellar Initial Mass Function*, eds. G. Gilmore and D. Howell, *A.S.P. Conf. Series*, 142:201–
- Shu, F.H. 1977. Self-similar collapse of isothermal spheres and star formation. *Astrophys. J.* 214:488–497
- Shu, F.H., Adams, F.C., and Lizano, S. 1987. Star formation in molecular clouds - Observation and theory. *Ann. Rev. Astron. Astrophys.* 25:23–81
- Shu, F., Najita, J., Galli, D., Ostriker, E., and Lizano S. 1993. The collapse of clouds and the formation and evolution of stars and disks. In *Protostars & Planets III*, eds. E. H. Levy and J. I. Lunine (Tucson: Univ. of Arizona Press), pp. 3–45.
- Shu, F.H., Najita, J., Ostriker, E., Wilkin, F., Ruden, S., and Lizano, S. 1994. Magnetocentrifugally driven flows from young stars and disks. I: A generalized model. *Astrophys. J.* 429:781–796

- Silk, J. 1995. A theory for the initial mass function. *Astrophys. J. Lett.* 438:L41–L44
- Sonnhalter, C., Preibisch, T., and Yorke, H.W. 1995. Frequency dependent radiation transfer in protostellar disks. *Astron. Astrophys.* 299:545–556
- Stahler S.W. 1988. Deuterium and the stellar birthline. *Astrophys. J.* 332:804–825
- Stahler, S.W., & Walter, F.M. 1993. Pre-main-sequence evolution and the birth population. In *Protostars & Planets III*, eds. E. H. Levy and J. I. Lunine (Tucson: Univ. of Arizona Press), pp. 405–428
- Stanke, T., McCaughrean, M., and Zinnecker, H. 1998. First results of an unbiased H₂ survey for protostellar jets in OrionA. *Astron. Astrophys.* 332:307–313
- Tafalla, M., Mardones, D., Myers, P.C., Caselli, P., Bachiller, R., and Benson, P.J. 1998. L1544: A Starless Dense Core with Extended Inward Motions. *Astrophys. J.* 504:900–914
- Tamura, M., Hayashi, S.S., Yamashita, T., Duncan, W.D., and Hough, J.H. 1993. Magnetic field in a low-mass protostar disk – Millimeter polarimetry of IRAS 16293-2422. *Astrophys. J. Lett.* 404:L21–L24
- Terebey, S., and Padgett, D.L. 1997. Millimeter interferometry of Class 0 sources: Rotation and infall towards L1448N. In *Herbig-Haro Flows and the Birth of Low Mass Stars. Proc. IAU Symp. 182*, eds. B. Reipurth and C. Bertout (Dordrecht: Kluwer), pp. 507–514.
- Terebey, S., Chandler, C.J., & André, P. 1993. The contribution of disks and envelopes to the millimeter continuum emission from very young low-mass stars. *Astrophys. J.* 414:759–772
- Terebey, S., Vogel S.N., Myers P.C. 1989. High-resolution CO observations of young low-mass stars. *Astrophys. J.* 340:472–478
- Testi, L., and Sargent, A.I. 1998. Star Formation in Clusters: A Survey of Compact Millimeter-Wave Sources in the Serpens Core. *Astrophys. J. Lett.* 508:L91–L94
- Tinney, C.G. 1993. The faintest stars - The luminosity and mass functions at the bottom of the main sequence. *Astrophys. J.* 414:279–301
- Tinney, C.G. 1995. The Faintest Stars: The Luminosity and Mass Functions at the Bottom of the Main Sequence – Erratum. *Astrophys. J.* 445:1017
- Tomisaka, K. 1996. Accretion in Gravitationally Contracting Clouds. *Publ. Astron. Soc. Japan* 48:L97–L101
- Umamoto, T., Iwata, T., Fukui, Y., Mikami, H., Yamamoto, S., Kameyama, O., and Hirano, N. 1992. The outflow in the L1157 dark cloud - Evidence for shock heating of the interacting gas. *Astrophys. J. Lett.* 392:L83–L86
- Velusamy, T., and Langer, W.D. 1998. Outflow-infall interactions

- as a mechanism for terminating accretion in protostars. *Nature* 392:685–687
- Walker, C.K., Adams, F.C., and Lada, C.J. 1990. 1.3 millimeter continuum observations of cold molecular cloud cores. *Astrophys. J.* 349:515–528
- Walker, C.K., Lada, C.J., Young, E.T., Maloney, P.R., & Wilking, B.A. 1986. Spectroscopic evidence for infall around an extraordinary IRAS source in Ophiuchus. *Astrophys. J. Lett.* 309:L47–L51
- Walker, C.K., Narayanan, G., & Boss, A.P. 1994. Spectroscopic signatures of infall in young protostellar systems. *Astrophys. J.* 431:767–782
- Ward-Thompson, D. 1996. The Formation and Evolution of Low Mass Protostars. *Astrophys. Space Sci.* 239: 151–170
- Ward-Thompson, D., Eiroa, C., and Casali, M.M. 1995. Confirmation of the driving source of the NGC 2264G bipolar outflow: a Class 0 protostar. *Mon. Not. Roy. Astron. Soc.* 273:L25–L28
- Ward-Thompson, D., Motte, F., and André, P. 1999. The initial conditions of isolated star formation. III: Millimetre continuum mapping of pre-stellar cores. *Mon. Not. Roy. Astron. Soc.* in press (WMA99)
- Ward-Thompson, D., Buckley, H.D., Greaves, J.S., Holland, W.S., and André, P. 1996. Evidence for protostellar infall in NGC 1333-IRAS2. *Mon. Not. Roy. Astron. Soc.* 281:L53–L56
- Ward-Thompson, D., Chini, R., Krugel, E., André, P., and Bontemps, S. 1995. A submillimetre study of the Class 0 protostar HH24MMS. *Mon. Not. Roy. Astron. Soc.* 274:1219–1224
- Ward-Thompson, D., Scott, P. F., Hills, R. E., and André, P. 1994. A submillimetre continuum survey of pre-protostellar cores. *Mon. Not. Roy. Astron. Soc.* 268:276–290
- White, G.J., Casali, M.M., and Eiroa, C. 1995. High resolution molecular line observations of the Serpens Nebula. *Astron. Astrophys.* 298:594–605
- Whitney, B.A., and Hartmann, L. 1993. Model scattering envelopes of young stellar objects. II - Infalling envelopes. *Astrophys. J.* 402:605–622
- Whitworth, A., and Summers, D. 1985. Self-similar condensation of spherically symmetric self-gravitating isothermal gas clouds. *Mon. Not. Roy. Astron. Soc.* 214:1–25
- Whitworth, A.P., Bhattal, A.S., Francis, N., and Watkins, S.J. 1996. Star formation and the singular isothermal sphere. *Mon. Not. Roy. Astron. Soc.* 283:1061–1070
- Wiesemeyer, H. 1997. The spectral signature of accretion in low-mass protostars. *Ph. D. Dissertation, University of Bonn*
- Wiesemeyer, H., Güsten, R., Wink, J.E., and Yorke, H.W. 1997. High resolution studies of protostellar condensations in NGC 2024. *As-*

- tron. Astrophys.* 320:287–299
- Wiesemeyer, H., Güsten, R., Cox, P., Zylka, R., and Wright, M.C.H. 1998. The Pivotal Onset of Protostellar Collapse: ISO's View and Complementary Observations. In *Star Formation with ISO*, eds. J.L. Yun & R. Liseau, *A.S.P. Conf. Series*, 132:189–194
- Wilking, B.A., Lada, C.J., & Young, E.T. 1989. IRAS observations of the Rho Ophiuchi infrared cluster - Spectral energy distributions and luminosity function. *Astrophys. J.* 340:823–852 (WLY89)
- Wilking, B.A., Schwartz, R.D., Fanetti, T.M., and Friel, E.D. 1997. Herbig-Haro Objects in the ρ Ophiuchi Cloud. *Publ. Astron. Soc. Pacific* 109:549–553
- Wilner, D.J., Welch, W.J., and Forster, J.R. 1995. Sub-Arcsecond Imaging of W3(OH) at 87.7 GHz. *Astrophys. J. Lett.* 449:L73–L76
- Wolf-Chase, G.A., Barsony, M., Wootten, H.A., Ward-Thompson, D., Lowrance, P.J., Kastner, J.H., and McMullin, J.P. 1998. The Protostellar Origin of a CS Outflow in S68N. *Astrophys. J. Lett.* 501:L193–L198
- Wood, D.O.S., Myers, P.C., & Daugherty, D. A. 1994. IRAS images of nearby dark clouds. *Astrophys. J. Sup.* 95:457–501
- Wootten, A. 1989. The Duplicity of IRAS 16293-2422: A Protobinary Star? *Astrophys. J.* 337:858–864
- Yorke, H. W., Bodenheimer, P., and Laughlin, G. 1995. The formation of protostellar disks. II: Disks around intermediate-mass stars *Astrophys. J.* 443:199–208
- Yu, K. C., Bally, J., and Devine, D. 1997. Shock-Excited H₂ Flows in OMC-2 and OMC-3. *Astrophys. J. Lett.* 485:L45–L48
- Yun, J. L., Moreira, M. C., Torrelles, J. M., Afonso, J. M., and Santos, N. C. 1996. A Search for Radio Continuum Emission From Young Stellar Objects in Bok Globules. *Astron. J.* 111:841–845
- Zavagno, A., Molinari, S., Tommasi, E., Saraceno, P., and Griffin, M. 1997. Young Stellar Objects in Lynds 1641: a submillimetre continuum study. *Astron. Astrophys.* 325:685–692
- Zhou, S., Evans II, N.J., Kömpe, C., & Walmsley, C.M. 1993. Evidence for protostellar collapse in B335. *Astrophys. J.* 404:232–246
- Zinnecker, H., Bastien, P., Arcoragi, J.P., & Yorke, H.W. 1992. Submillimeter dust continuum observations of three low luminosity protostellar IRAS sources. *Astron. Astrophys.* 265:726–732
- Zinnecker, H., McCaughrean, M.J., and Rayner, J.T. 1998. A symmetrically pulsed jet of gas from an invisible protostar in Orion. *Nature* 394:862–865

FIGURE CAPTIONS

Figure 1. Dust continuum images of L1544 at 90 μm (a) and 200 μm (b) from ISOPHOT, at 850 μm (c) from SCUBA, and at 1.3 mm (d) from IRAM 30 m. A polarization E-vector, perpendicular to the B field, is overlaid on the 850 μm image (c), as measured with the SCUBA polarimeter. The observed morphology is consistent with a magnetically-supported core that has flattened along the direction of the mean magnetic field.

Figure 2. Spectral energy distributions of the pre-stellar core L1544 and the Class 0 protostar IRAS 16293, along with grey-body fits (see text). The L1544 SED is based on ISOPHOT, JCMT, and IRAM data from Ward-Thompson et al. (1999a,b). The IRAS 16293 SED is based on IRAS, ISO-LWS (Correia, Griffin et al. 1999 in prep. – see also Ceccarelli et al. 1998), and JCMT data (Sandell 1994). Note that a simple grey-body model cannot account for the 25 μm emission of IRAS 16293 and that a two-component model is required (Correia et al. 1999).

Figure 3. (a) (left) Radial intensity profile of L1689B at 1.3 mm illustrating that pre-stellar cores have flat inner density profiles (from André, Ward-Thompson, & Motte 1996). For comparison, the dotted curve shows a spherical isothermal model with $\rho(r) \propto r^{-1.2}$ for $r < 4000$ AU and $\rho(r) \propto r^{-2}$ for $r \geq 4000$ AU. The dash-dotted curve shows a model with $\rho(r) \propto r^{-2}$ such as a singular isothermal sphere (SIS).

(b) (right) Typical density profiles expected for a magnetically supported core undergoing ambipolar diffusion at various times increasing from t_0 to t_6 (from Ciolek & Mouschovias 1994). The normalization values are $n_{n,c0} = 2.6 \times 10^3 \text{ cm}^{-3}$ and $R_0 = 4.29 \text{ pc}$. Open circles mark the instantaneous radius of the uniform-density central region; starred circles mark the radius of the magnetically supercritical region (present only for $t \geq t_2$).

Figure 4. Plot of lifetime vs. mean density for six core samples compared with $t \propto \rho^{-0.75}$ and $t \propto \rho^{-0.5}$ as predicted by ambipolar diffusion models with different ionisation mechanisms (Jessop & Ward-Thompson 1999).

Figure 5. Dust continuum mosaic of the ρ Oph cloud taken at 1.3 mm with the IRAM 30m telescope and the MPIFR bolometer array (Motte, André, & Neri 1998).

Figure 6. Mass spectrum of the 59 pre-stellar fragments extracted from the ρ Oph 1.3 mm continuum mosaic shown in Fig. 5 (from Motte et al. 1998). For comparison, dotted and long-dashed lines show power laws of the form $\Delta N/\Delta M \propto M^{-1.5}$ and $\Delta N/\Delta M \propto M^{-2.5}$, respectively. This pre-stellar mass spectrum is remarkable in that it resembles the shape of the IMF.

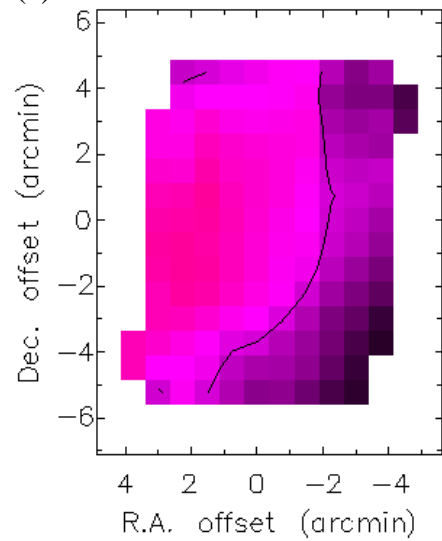
Figure 7. (a) $L_{bol}-T_{bol}$ diagram for 14 well-documented YSOs along with three model evolutionary tracks for various (final) stellar masses and cloud temperatures (from Myers et al. 1998). Four times t (Myr) since the start of infall are indicated, at $\log t = -1.5, -1.0, -0.5,$ and 0.0 .

(b) $M_{env}-L_{bol}$ diagram for a sample of Class I (filled circles) and confirmed Class 0 sources (open circles) mainly in Ophiuchus, Perseus, and Orion (adapted from AM94 and Saraceno et al. 1996a). Evolutionary tracks, computed assuming protostars form from bounded condensations of finite initial masses and have $L_{bol} = GM_{\star}M_{acc}/R_{\star} + L_{\star}$, where L_{\star} is

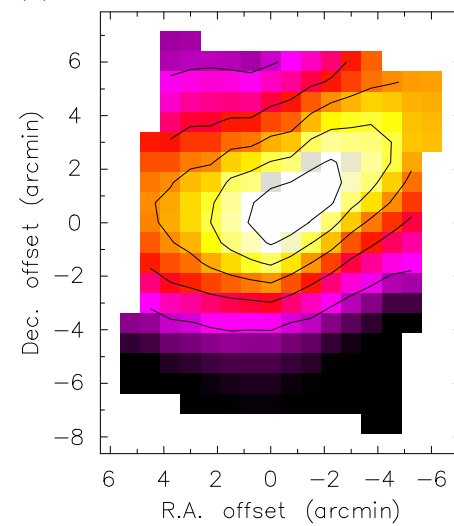
the PMS birthline luminosity (e.g. Stahler 1988), are shown. M_{env} and $\dot{M}_{\text{acc}} = M_{\text{env}}/\tau$ (where $\tau = 10^5$ yr) have been assumed to decline exponentially with time (see Bontemps et al. 1996a). Small arrows are plotted on the tracks every 10^4 yr, big arrows when 50% and 90% of the initial condensation has been accreted. The dashed and dotted lines are two M_{\star} – L_{bol} relations marking the conceptual border zone between the Class 0 ($M_{\text{env}} > M_{\star}$) and the Class I ($M_{\text{env}} < M_{\star}$) stage; the dashed line has $M_{\star} \propto L_{\text{bol}}$ (cf. AWB93 and AM94) while the dotted line has $M_{\star} \propto L_{\text{bol}}^{0.6}$ as suggested by the accretion scenario adopted in the tracks.

Figure 8. Normalized outflow momentum flux, $F_{\text{CO}} c/L_{\text{bol}}$, versus normalized envelope mass, $M_{\text{env}}/L_{\text{bol}}^{0.6}$, for a sample of Class 0 (open circles) and Class I (filled circles) objects (from Bontemps et al. 1996a). $F_{\text{CO}} c/L_{\text{bol}}$ can be taken as an empirical tracer of the accretion rate \dot{M}_{acc} , while $M_{\text{env}}/L_{\text{bol}}^{0.6}$ is an evolutionary indicator which decreases with time. This diagram should therefore mainly reflect the evolution of \dot{M}_{acc} during the protostellar phase. The solid curve shows the accretion rate history predicted by the simplified collapse model of Henriksen et al. (1997).

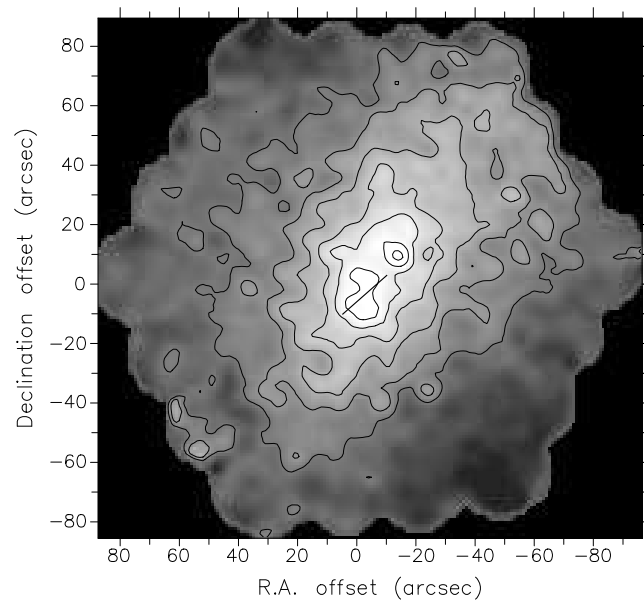
(a) L1544 at 90 microns



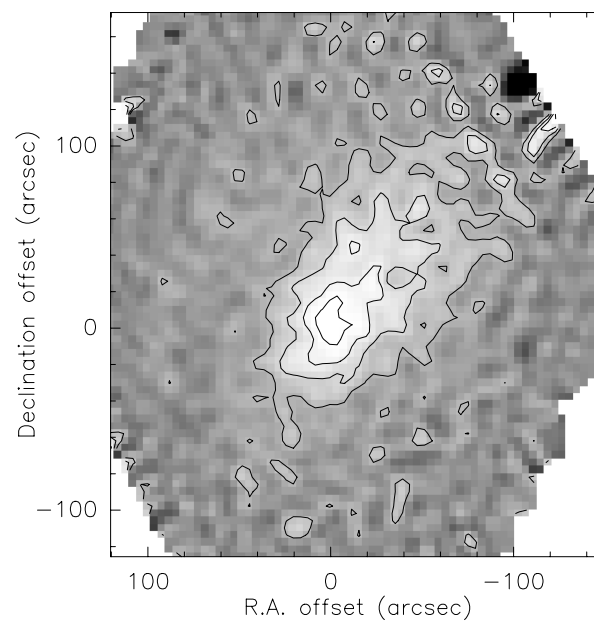
(b) L1544 at 200 microns

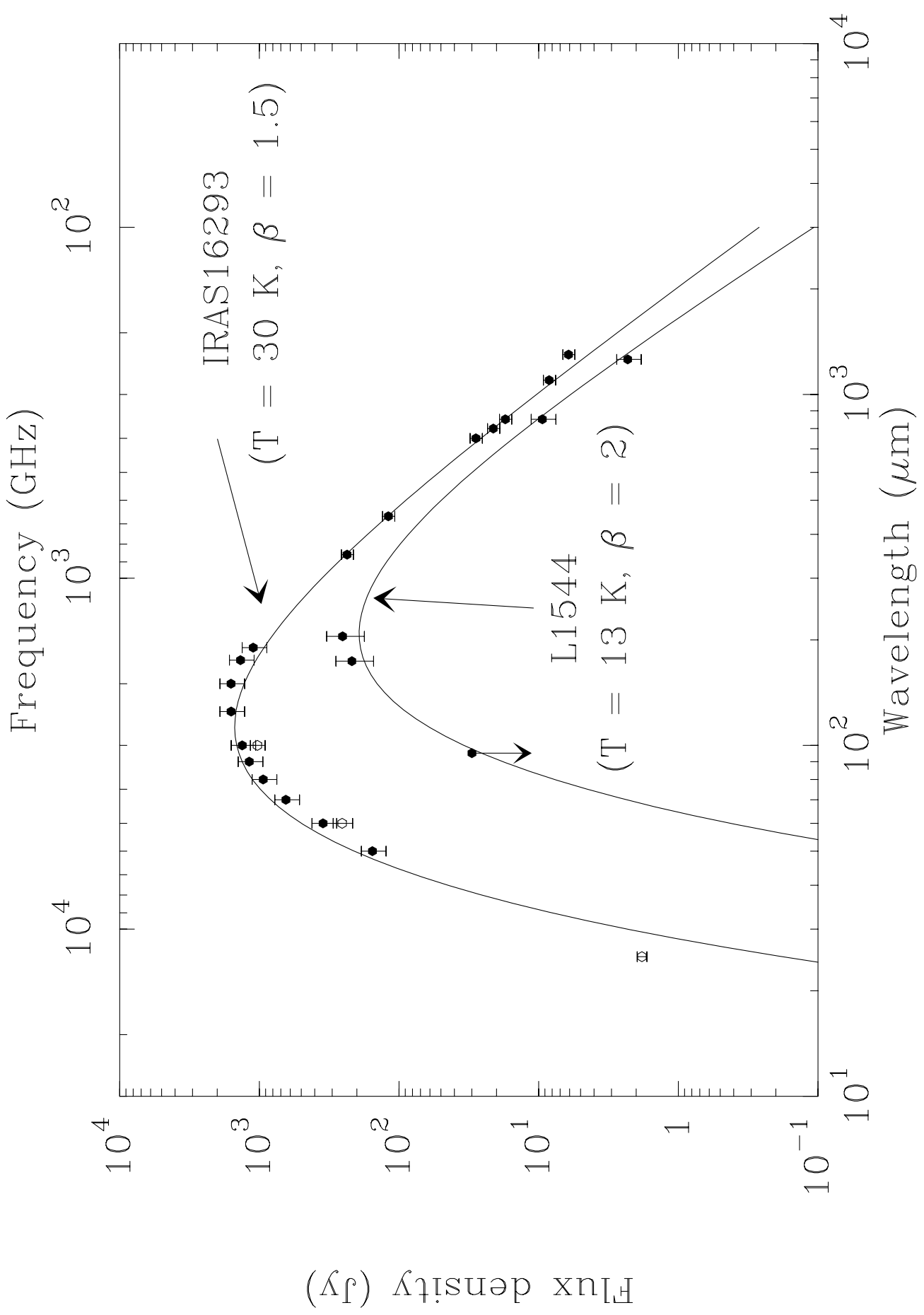


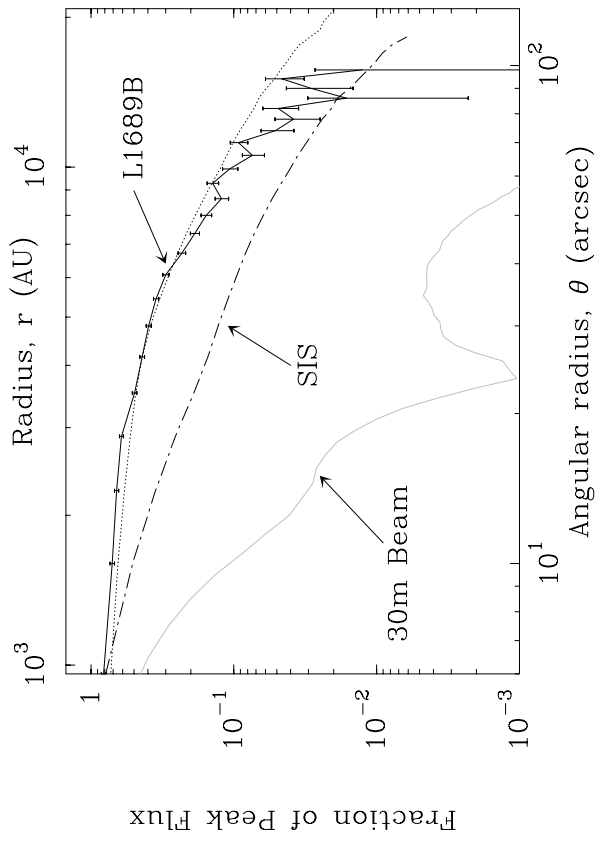
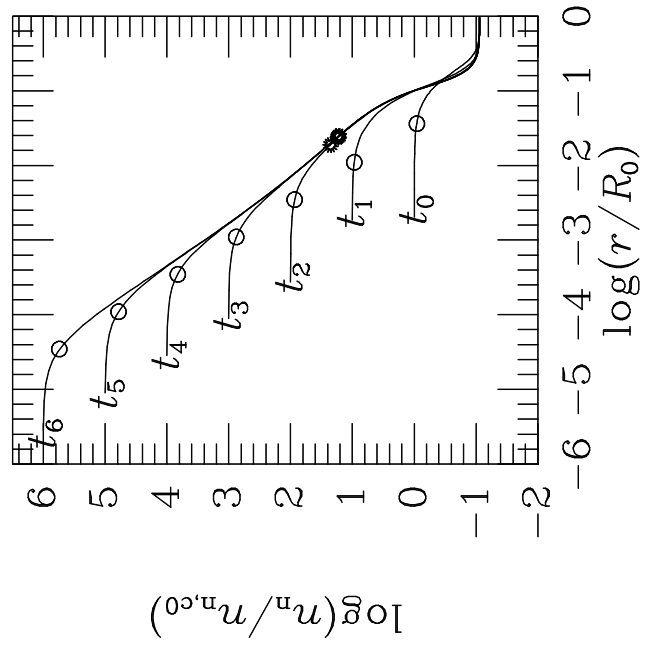
(c) L1544 at 850 microns



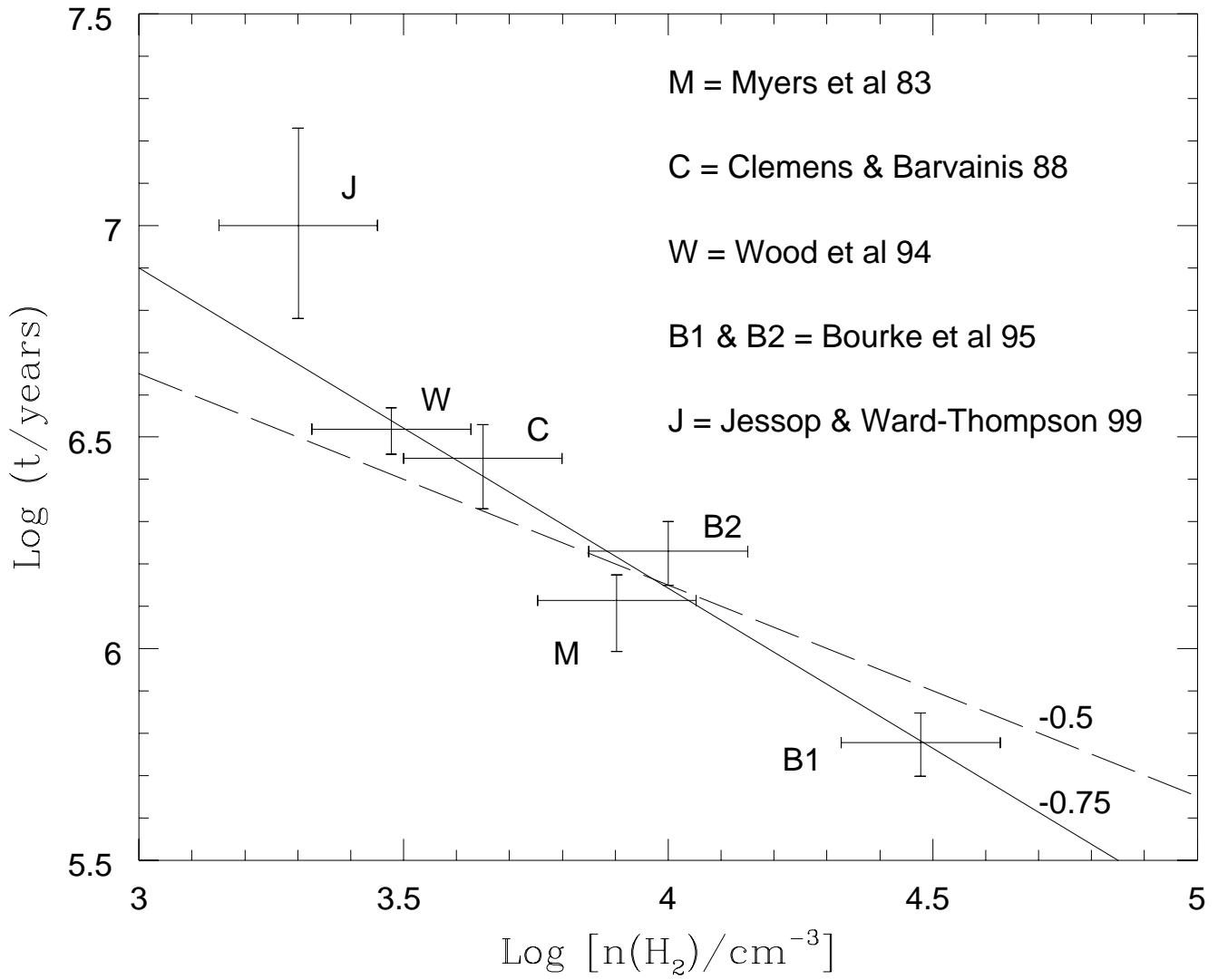
(d) L1544 at 1.3 mm



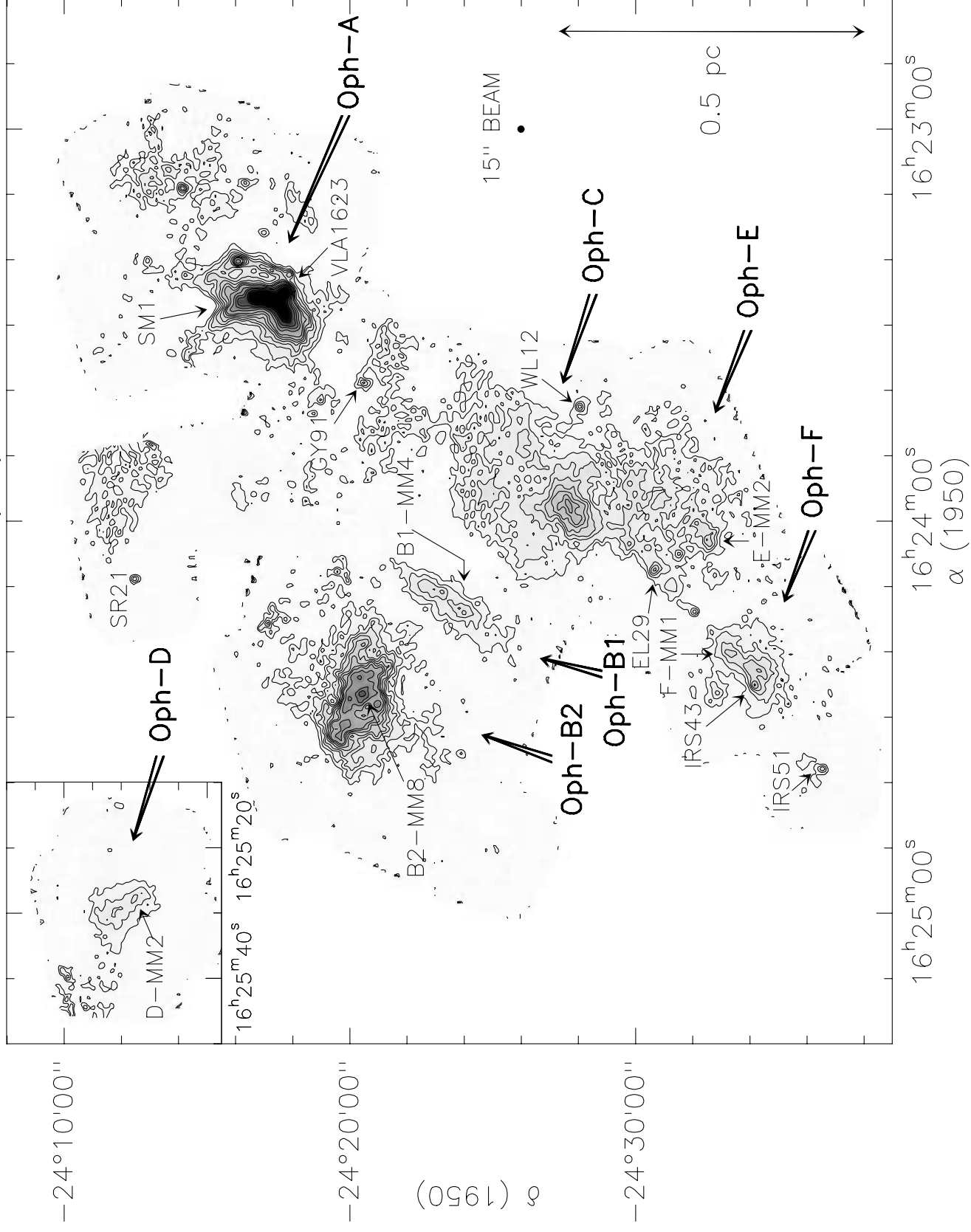


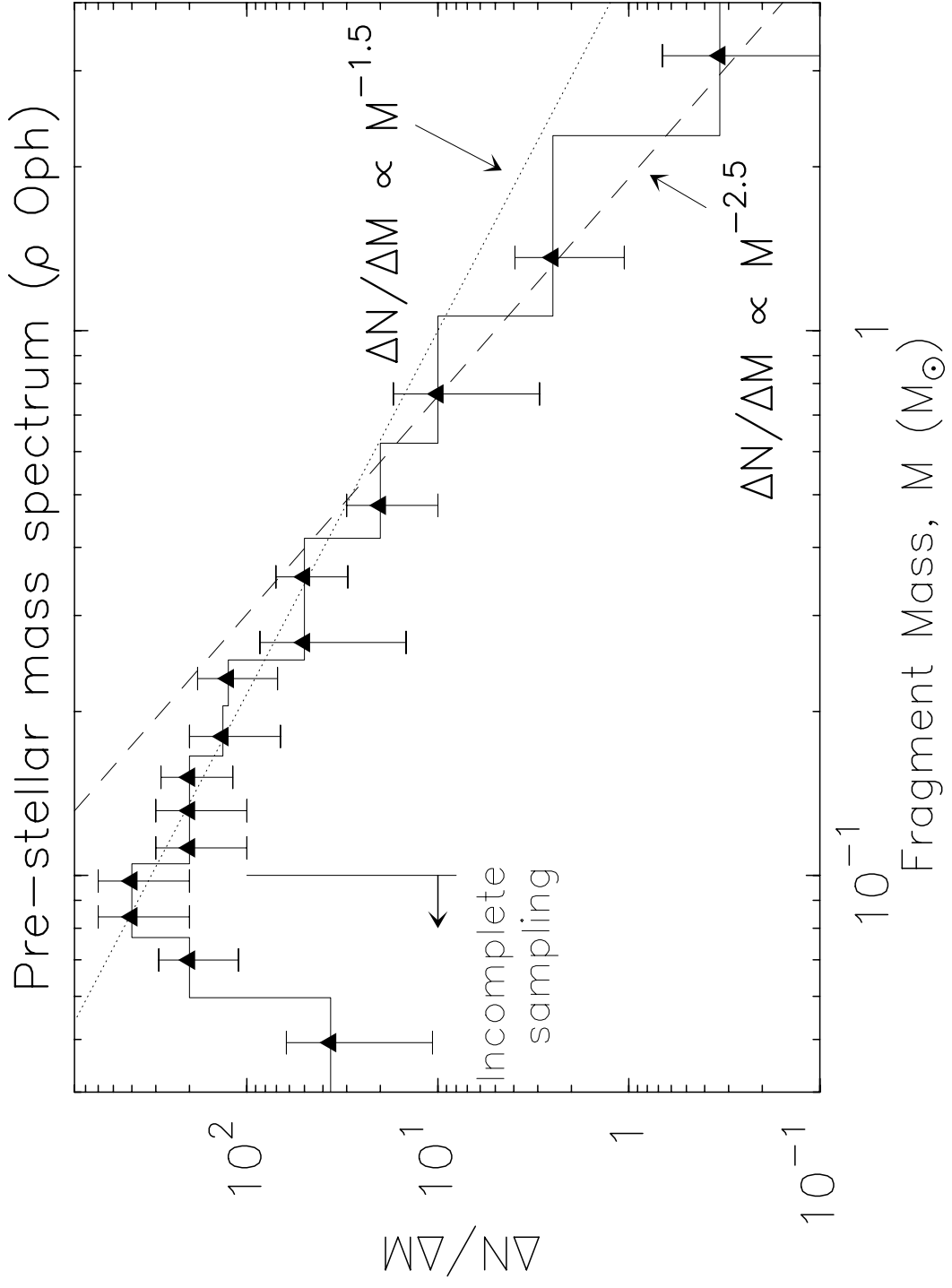


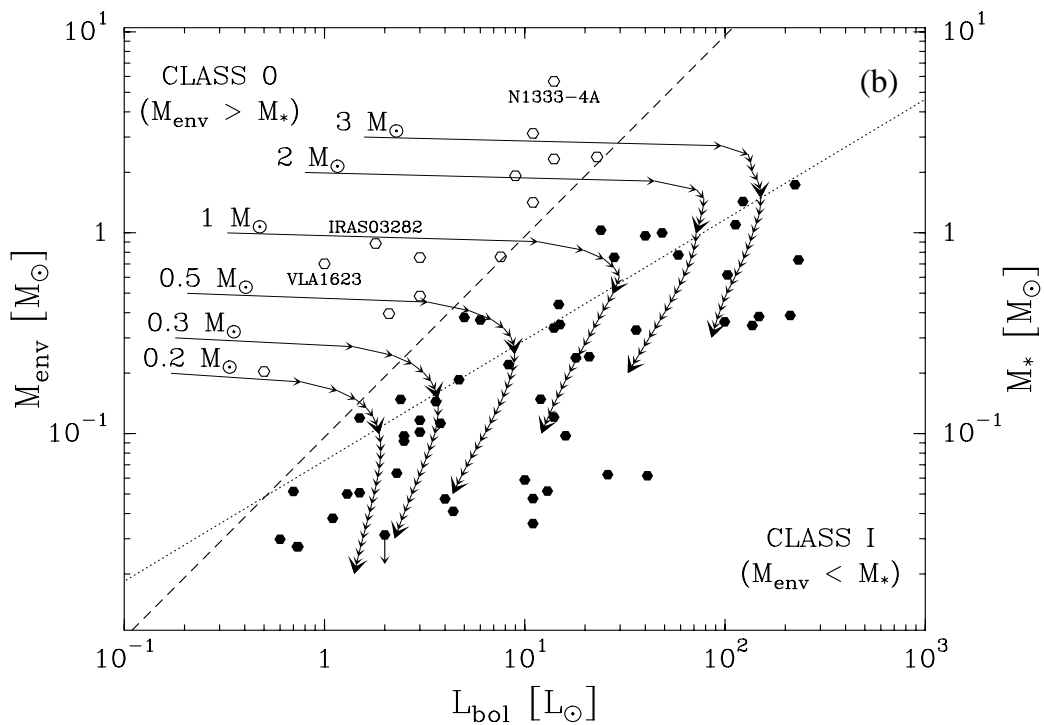
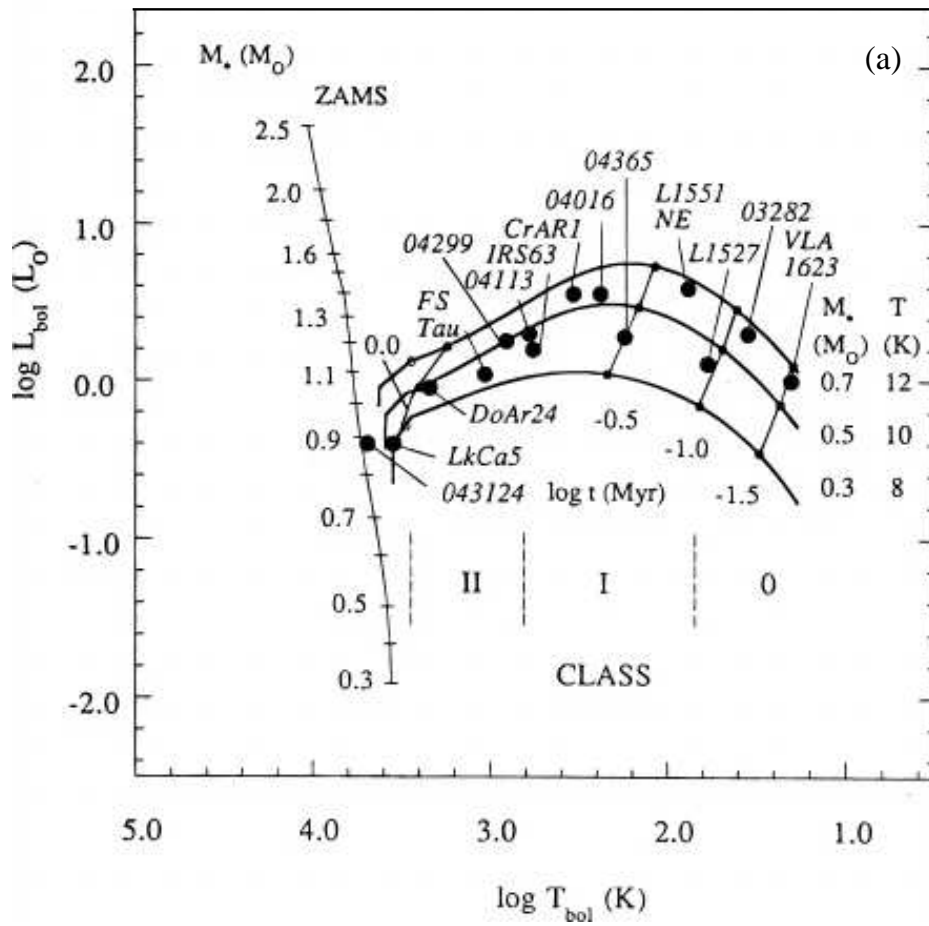
CORE LIFETIME vs DENSITY



1.3mm mosaic of ρ Oph main cloud







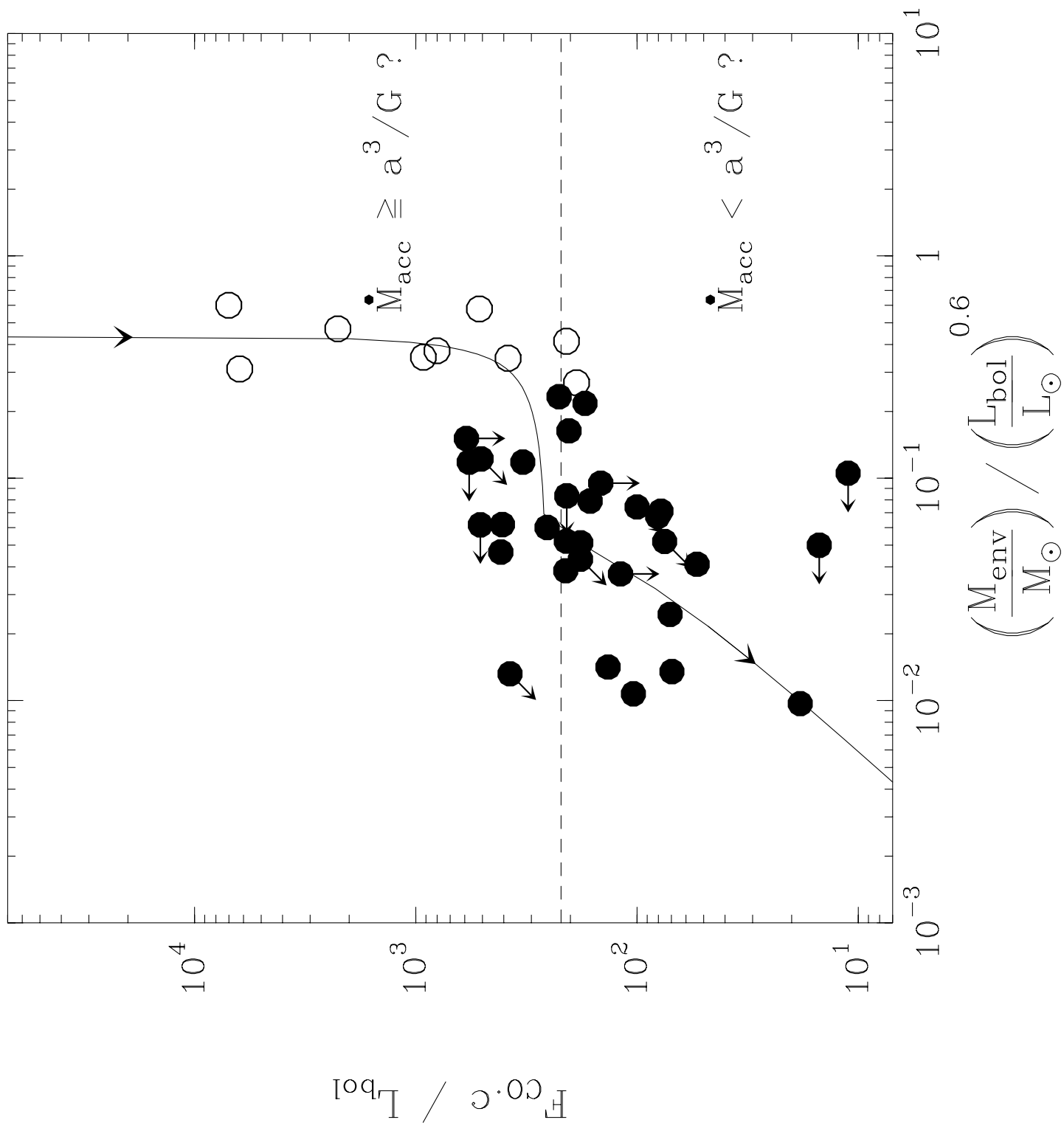


Table 1: Properties of confirmed Class 0 protostars

Object	$\alpha(2000)$	$\delta(2000)$	Dist. (pc)	L_{bol} (L_{\odot})	M_{env} (M_{\odot})	L_{smm}/L_{bol} (%) ^a	T_{bol} (K)	Outflow Manifestations	Infall	Struc- ture ^b	References
W3OH-TW [†]	02:27:04.7	+61:52:24	2200	10^3-10^4	~ 20	~ 1	$\gtrsim 80?$	H ₂ O, radio	—	—	1
L1448-IRS2	03:25:22.4	+30:45:12	300	6	0.9	3	70?	CO	—	—	2
L1448-N	03:25:36.3	+30:45:15	300	11	2.3	3	70	CO, radio	Y?	D, B	3,4,5,6,7,8,9,10
L1448-C	03:25:38.8	+30:44:05	300	9	1.4	2	60	CO, radio, H ₂	N?	D	3,4,5,11,12,8,10,13
NGC1333-IRAS2	03:28:55.4	+31:14:35	350	40	1.7	$\lesssim 1$	50	CO, H ₂	Y?	—	14,15,9,16,17,13
SVS13B	03:29:03.1	+31:15:52	350	~ 7	2.7	~ 5	~ 30	SiO, H ₂	—	—	18,19,20,21,22
NGC1333-IRAS4A	03:29:10.3	+31:13:31	350	14	7.	5	34	CO, radio	Y	D, B	23,24,15,16,25,26,27,28,10,13
NGC1333-IRAS4B	03:29:12.0	+31:13:09	350	14	2.7	3	36	CO, radio	Y	D, B	23,24,15,16,25,28,10,13
IRAS 03282	03:31:20.8	+30:45:31	300	1.5	0.6	5	35	CO, H ₂	—	—	29,30,8
HH211-MM	03:43:56.8	+32:00:50	300	5	1.5	~ 4	~ 30	H ₂	—	—	31,32
IRAM 04191	04:21:56.9	+15:29:46	140	0.15	0.5	12	18	CO, radio	Y	N?	33
L1527 [†]	04:39:53.9	+26:03:10	140	2	0.4	0.7	60	CO, H ₂	Y	D	34,35,36,37,38,6,10,13
HH114MMS	05:18:15.2	+07:12:03	450	$\lesssim 25$	2.8	$\gtrsim 1$	~ 40	radio, HH	—	—	19
RNO43-MM	05:32:19.4	+12:49:42	400	5	0.6	~ 5	36	CO, radio, H ₂	N?	—	39,19,40,41,10
OMC3-MM6	05:35:23.5	-05:01:32	450	< 60	12	$\gtrsim 2$	~ 30	CO, H ₂	—	—	42,43
L1641-VLA1 [†]	05:36:22.8	-06:46:07	450	50	6.5	~ 3	70?	radio, HH	—	—	44,19,45
NGC2023-MM1	05:41:24.8	-02:18:09	450	~ 8	1.8-4.6	$\sim 3-10$	~ 30	CO	—	—	46,47
NGC2024-FIR5	05:41:44.5	-01:55:43	450	$\gtrsim 10$	15.	$\lesssim 30$	20	CO	N?	D, B?	48,49,50,10
NGC2024-FIR6	05:41:45.2	-01:56:05	450	$\gtrsim 15$	6.	$\lesssim 10$	20	CO	N?	—	48,49,50,10
HH212-MM	05:43:51.5	-01:02:52	400	14	1.2	~ 2	70?	CO, H ₂	—	—	39,19,51
HH24MMS	05:46:08.3	-00:10:42	450	5	4	10	20?	radio, H ₂	—	D	52,53,54,55,9,56
HH25MMS [†]	05:46:07.5	-00:13:36	450	6	0.5	5	34	CO, radio, H ₂	Y?	—	54,57,10
NGC2264G-VLA2	06:41:11.1	+09:55:59	800	12	2	2	25	CO, radio	—	—	58,59,60
IRAS 08076 [†]	08:09:32.8	-36:05:00	400	17	2.3	$\gtrsim 1$	74	CO, H ₂	—	—	61,16,62
BHR71-MM	12:01:36.3	-65:08:44	200	10	2.4	~ 3	56	CO, HH	—	—	63,62
IRAS 13036 [†]	13:07:36.1	-77:00:05	200	1.7	0.3	$\lesssim 2$	60	CO	Y	—	62,64,13
VLA 1623	16:26:26.4	-24:24:30	160	1	0.7	10	< 35	CO, radio, H ₂	Y?	D, B?	65,66,67,68,69,70,9,10,13,71,22
IRAS 16293	16:32:22.7	-24:28:32	160	23	2.3	2	43	CO, radio	Y	D, B	72,73,74,75,26,27,76,77,10,13
Trifid-TC3 [‡]	18:02:07.0	-23:05:11	1680	$\sim 10^3$	~ 60	~ 1	~ 30	SiO	—	—	78
L483-MM [†]	18:17:29.8	-04:39:38	200	9	0.3	~ 0.7	50	CO, radio	Y?	—	79,37,10,13
Serp-S68N	18:29:47.9	+01:16:46	310	6	1.0	3	40?	CO, CS	Y?	—	80,81,82,83,84,13
Serp-FIRS1 [†]	18:29:49.9	+01:15:20	310	46	3	~ 1	51	CO, radio	N?	N?	85,80,81,82,86,84,10,13,87

Table 1 (cont'd)

Object	$\alpha(2000)$	$\delta(2000)$	Dist. (pc)	L_{bol} (L_{\odot})	M_{env} (M_{\odot})	L_{smm}/L_{bol} (%) ^a	T_{bol} (K)	Outflow Manifestations	Infall	Struc- ture ^b	References
Serp-SMM4	18:29:57.1	+01:13:15	310	9	3	~ 3	35	CO, radio	Y	N?	85,81,82,84,88,10,13,87
Serp-SMM3 [†]	18:29:59.7	+01:14:00	310	8	0.9	~ 1	40	CO, H ₂	N?	N?	85,81,82,84,89,10,87
G34.24+0.13MM [‡]	18:53:21.5	+01:13:45	3700	4000	100	~ 0.5	50	CH ₃ OH	–	–	90
L723-MM	19:17:53.7	+19:12:20	300	3	0.6	~ 4	50	CO, radio	N?	–	91,92,32,19,93,94,10
B335	19:37:00.8	+07:34:11	250	3	0.8	6	37	CO, radio	Y	D?	91,95,96,40,97,10,13,98
S106-SMM	20:27:25.3	+37:22:46	600	$\gtrsim 24$	$\lesssim 10$	$\lesssim 8$	$\gtrsim 20$	bip. HII, H ₂ O	–	–	99,70
L1157-MM	20:39:06.2	+68:02:22	440	11	0.5	~ 5	~ 60	CO, H ₂	Y	D?	100,32,101,69,10,13
GF9-2	20:51:30.1	+60:18:39	200	0.3	~ 0.5	~ 10	$\lesssim 20$	–	Y	–	102,103,104
CepE-MM	23:03:13.1	+61:42:26	730	75	7	~ 2	~ 60	CO, H ₂	–	–	105,106
IRAS 23385 [‡]	23:40:54.5	+61:10:28	4900	16000	370	~ 0.7	$\gtrsim 40$	SiO	–	–	107

^a L_{smm} is the luminosity radiated longward of 350 μm ; Class 0s are defined by $L_{smm}/L_{bol} > 0.5\%$ (see III-A).

^b Small-scale structure: D = presence of disk-like component; B = binary or multiple system; N = single object with no disk

[†] Border-line Class 0. [‡] Candidate massive Class 0 object.

References: (1) Wilner et al. 1995; (2) O’Linger et al. 1998; (3) Bachiller et al. 1990; (4) Curiel et al. 1990; ; (5) Bachiller et al. 1995; (6) Terebey et al. 1993; (7) Terebey & Padgett 1997; (8) Barsony et al. 1998; (9) Greaves et al. 1997; (10) Gregersen et al. 1997; (11) Bachiller et al. 1991a; (12) Bally et al. 1993; (13) Mardones et al. 1997; (14) Sandell et al. 1994; (15) Langer et al. 1996; (16) Hodapp & Ladd 1995; (17) Ward-Thompson et al. 1996; (18) Grossman et al. 1997; (19) Chini et al. 1997a; (20) Bachiller et al. 1998; (21) Lefloch et al. 1998; (22) Looney et al. 1999; (23) Sandell et al. 1991; (24) Blake et al. 1995; (25) Mundy et al. 1993; (26) Akeson & Carlstrom 1997; (27) Greaves & Holland 1998; (28) Lay et al. 1995; (29) Bachiller et al. 1991b; (30) Bachiller et al. 1994; (31) McCaughrean et al. 1994; (32) Motte 1998; (33) André et al. 1999; (34) Ladd et al. 1991; (35) Eiroa et al. 1994; (36) Bontemps et al. 1996a; (37) Myers et al. 1995; (38) Ohashi et al. 1997; (39) Zinnecker et al. 1992; (40) Anglada et al. 1992; (41) Bence et al. 1996; (42) Chini et al. 1997b; (43) Yu et al. 1997; (44) Pravdo et al. 1985; (45) Zavagno et al. 1997; (46) Sandell et al. 1999; (47) Launhardt et al. 1996; (48) Mezger et al. 1992; (49) Richer et al. 1992; (50) Wiesemeyer et al. 1997; (51) Zinnecker et al. 1998; (52) Chini et al. 1993; (53) Ward-Thompson et al. 1995a; (54) Bontemps et al. 1995; (55) Bontemps et al. 1996b; (56) Chandler et al. 1995; (57) Gibb & Davis 1998; (58) Gómez et al. 1994; (59) Ward-Thompson et al. 1995b; (60) Lada & Fich 1996; (61) Persi et al. 1994; (62) Henning & Launhardt 1998; (63) Bourke et al. 1997; (64) Lehtinen 1997; (65) André et al. 1990; (66) AWB93; (67) Leous et al. 1991; (68) Dent et al. 1995; (69) Davis & Eislöffel 1995; (70) Holland et al. 1996; (71) Pudritz et al. 1996; (72) Walker et al. 1986; (73) Wootten 1989; (74) Mizuno et al. 1990; (75) Tamura et al. 1993; (76) Mundy et al. 1992; (77) Walker et al. 1994; (78) Cernicharo et al. 1998; (79) Fuller et al. 1995a; (80) McMullin et al. 1994; (81) Hurt & Barsony 1996; (82) White et al. 1995; (83) Wolf-Chase et al. 1998; (84) Hurt et al. 1996; (85) Casali et al. 1993; (86) Curiel et al. 1993; (87) Hogerheijde et al. 1999; (88) Bontemps 1996; (89) Herbst et al. 1997; (90) Hunter et al. 1998; (91) Davidson 1987; (92) Cabrit & André 1991; (93) Anglada et al. 1991; (94) Avery et al. 1990; (95) Chandler et al. 1990; (96) Cabrit et al. 1988; (97) Zhou et al. 1993; (98) Hirano et al. 1992; (99) Richer et al. 1993; (100) Umemoto et al. 1992; (101) Gueth et al. 1997; (102) Güsten 1994; (103) Wiesemeyer 1997; (104) Wiesemeyer et al. 1998; (105) Lefloch et al. 1996; (106) Ladd & Hodapp 1997; (107) Molinari et al. 1998.